ABSTRACT

Title of Thesis: THE IMPACTS OF BRANCED CHAIN AMINO ACID SUPPLEMENTATION ON ADIPOCYTE FUNCTION

Tabitha Mozelle Gregory
Master of Science, 2021

Thesis Directed By: Assistant Professor, Dr. Nishanth E. Sunny,
Department of Animal and Avian Sciences

The branched chain amino acids (BCAAs) are three essential amino acids: valine, leucine, and isoleucine. Adipose tissue has high rates of BCAA degradation and this has been shown to fuel normal function. Recent literature highlights cross-talk between BCAAs, lipid metabolism, and mitochondrial dysfunction. The objective of this thesis is to determine the impact of BCAA supplementation on adipose development, morphology, and various aspects of energy metabolism including BCAA degradation and lipolysis.

C57-BL6N mice were reared on either low-fat (LF), LF with 150% BCAAs (LB), high-fat (HF), or HF with 150% BCAAs (HB) diets for 12-34 weeks. Adipose tissue morphology and energetics were determined.

Results demonstrated that BCAA supplementation reduced lipid storage in visceral adipose depots, lowered circulating leptin, and reduced lipid accumulation in brown adipose tissue. BCAA supplementation also induced lipolysis, which raised circulating fatty acids. These results could have implications in the treatment and prevention of metabolic diseases.

THE IMPACTS OF BRANCHED CHAIN AMINO ACID SUPPLEMENTATION ON ADIPOCYTE FUNCTION

by

Tabitha Mozelle Gregory

Thesis submitted to the Faculty of the Graduate School of the
University of Maryland, College Park, in partial fulfillment
of the requirements for the degree of
Master of Science
2021

Advisory Committee:
Assistant Professor, Dr. Nishanth E. Sunny, Chair
Associate Professor, Dr. Byung-Eun Kim
Professor, Dr. Richard Kohn

Dedication

To my parents, Cecilia and Stephen, my family, and my fiancé Kyle. Thank you for all of your support and encouragement!

Dr. Sunny, thank you for your guidance, patience, and wisdom!

To my lab members, I will always be thankful for your help, contributions, and for lending a listening ear when I needed it!

Table of Contents

Dedication ii
Table of Contents iii
List of Tables iv
List of Figures v
Chapter 1: Introduction 1
Chapter 2: Literature Review 4
Branched Chain Amino Acids and Insulin Action 4
Tissue BCAA Degradation Pathways 5
Normal Adipose Tissue Function and Physiology in White and Brown Adipose Tissue 6
Adipose as a Endocrine Organ 10
Factors Influencing Adipose Expansion and Differentiation 11
Adipocyte Differentiation 12
Adipose Tissue and Lipid Metabolism 12
Evidence of BCAAs and Adipose Tissue Expansion and Differentiation 14
Evidence of BCAAs and Adipose Tissue Lipolysis 14
Adipose Tissue, BCAA degradation, and Mitochondrial Function 15
Chapter 3: Experimental Design and Methods 17
Animals 17
In-Vitro Lipolysis Assay 19
Analysis of Non-Esterified Fatty Acids (NEFA) 25
Analysis of Glycerol in Lipolysis Incubation Media 25
Western Blot Analysis of Adipose Tissue Proteins 25
Measurement of Circulating Biomarkers 28
Gene Expression Profiles 28
Adipose Histology 29
GC-MS Metabolomics 31
Statistical Analysis 31
Chapter 4: Results 34
Objective 1:The Impact of BCAAS on Adipose Tissue Morphology and Development 35
Objective 2: BCAA Degradation and Mitochondrial Function 48
Objective 3: Impact of BCAAs on Lipolysis 61
Chapter 5: Discussion 66
Impacts of BCAA Supplementation on Adipose Tissue Morphology and Development 66
BCAA Degradation and Mitochondrial Function 71
Impacts of BCAA supplementation on Adipose Tissue Lipolysis 73
Summary 75
Future Directions 75
Bibliography 77

List of Tables

Table 1- Custom mouse diet compositions

Table 2- *In vitro* lipolysis assay treatments

Table 3- Custom adipose explant media composition

Table 4- Non-essential amino acid stock composition

Table 5- BCAA stock composition

Table 6- 1x RIPA lysis buffer composition

Table 7- Mouse gene primer sequences

Table 8- Organic acid stable isotope internal standard

Table 9- Amino acid stable isotope internal standard

Table 10- Keto acid stable isotope internal standard

Table 11- Serum insulin and c-peptide concentrations

Table 12- Serum hormone analysis

List of Figures

Figure 1- Structures of the BCAAs

Figure 2- BCAA degradation pathways

Figure 3- Murine adipose depots

Figure 4- Comparative adipose histology

Figure 5- Adipocyte lipid metabolism

Figure 6- Roles of adipocyte mitochondria

Figure 7- Body and adipose weights

Figure 8- Adipose depot weights

Figure 9- LF and LF feed intake and body weights (12 weeks)

Figure 10- LF and LB feed intake and body weights (34 weeks)

Figure 11- HF and HB feed intake and body weights (12 weeks)

Figure 12- HF and HB feed intake and body weights (24 weeks)

Figure 13- WAT histology

Figure 14- BAT histology

Figure 15- WAT amino and keto acids metabolomic analysis

Figure 16- WAT gene expression

Figure 17- WAT organic acids metabolomic analysis

Figure 18- LF and LB WAT OXPHOS and COXIV protein expression

Figure 19- HF and HB WAT OXPHOS and COXIV protein expression

Figure 20- BAT amino and keto acids metabolomic analysis

Figure 21- BAT gene expression

Figure 22- BAT organic acids metabolomic analysis

Figure 23- LF and LB BAT OXPHOS and COXIV protein expression

Figure 24- HF and HB BAT OXPHOS and COXIV protein expression

Figure 25- Serum non-esterified fatty acid concentrations

Figure 26- Fatty acid and glycerol concentrations from *in-vitro* lipolysis assay media

Figure 27- BCAA-treated lipolysis assay

Figure 28- BCAA stimulated lipolysis assay

Chapter 1: Introduction

The branched chain amino acids (BCAAs) are three essential amino acids, Valine, Leucine, and Isoleucine, and are well known for their regulatory effects on protein, glucose, and lipid homeostasis in a variety of tissues. The BCAAs and their degradation are very responsive to the actions of insulin, and as such, defects in BCAA metabolism are central to the etiology of insulin resistant states including obesity, type II diabetes mellitus (T2DM), and non-alcoholic fatty liver disease (NAFLD). Additionally, degradation products of BCAA metabolism are anaplerotic substrates for the mitochondrial tri-carboxylic acid (TCA) cycle. Therefore, BCAAs can modulate mitochondrial function by impacting the TCA cycle activity and its intermediates. Similarly, the BCAAs also have potent signaling functions through their interactions with several molecular regulators of mitochondrial function (Neinast et al., 2019; Ye et al., 2020). Taken together, impairments in both BCAA catabolism and mitochondrial function are evident in insulin resistant tissues, and are characteristic features of obesity, NAFLD, and T2DM (Bjørndal et al., 2011; Gannon et al., 2018). Therefore, understanding the link between BCAAs, their degradation networks, and mitochondrial dysfunction at a tissue and cellular level is an area of significant interest for the study and management of metabolic diseases.

The BCAAs are major metabolic substrates for adipose tissue, which plays a crucial role in whole body BCAA degradation and clearance. Adipose tissue does this by using BCAAs as substrates for metabolite synthesis, energy, and heat production. For example, BCAAs are catabolized and utilized by maturing white adipose tissue

(WAT) to form new lipids (Estrada-Alcalde, Isabela et al., 2016). In murine brown adipose tissue (BAT) during cold challenges, mitochondria extensively utilize BCAAs as metabolic substrates for non-shivering thermogenesis (Yoneshiro et al., 2019). The utilization of BCAAs in WAT and BAT promote effective clearance of circulating BCAAs from the system. Defects in the ability of adipose tissue to efficiently catabolize BCAAs during the progressive severity of insulin resistance is thought to contribute to the increase of circulating levels of BCAAs, which is robustly correlated to indices of insulin resistance and is used as a clinical indicator for the development of insulin resistance (Nie et al., 2018).

BCAAs have also been shown to impact adipocytes through their ability to modulate adipocyte differentiation, mechanisms of lipid storage, and rates of lipolysis. In support of this, BCAA deprivation resulted in blunted adipocyte differentiation (Estrada-Alcalde, Isabela et al., 2016). Furthermore in growing swine, excessive BCAAs lead to an increase in the rate of adipose lipolysis (Heng et al., 2020). The multiple interactions between the BCAAs and various facets of adipose tissue function clearly illustrate the significant role of the BCAAs in maintaining the metabolic health of the adipose tissue.

Based on the above observations, we hypothesized that chronic, dietary supplementation of BCAAs will impact adipocyte function in WAT and BAT. We further hypothesized that this BCAA mediated induction of WAT and BAT function will be blunted during whole body insulin resistance.

We tested our hypothesis in mice reared on a low-fat or high-fat diets supplemented with either 150% excess or normal levels of BCAAs. The following were the objectives of this study:

1) To determine the impact of BCAAs on adipose tissue development and morphology during normal and insulin resistant states.

2) To determine the impact of BCAA supplementation on BCAA degradation and mitochondrial function in WAT and BAT during normal and insulin resistant states.

3) To determine the impact of BCAAs on rates of lipolysis in WAT during normal and insulin resistant states.

Chapter 2: Literature Review

Branched Chain Amino Acids and Insulin Action

Valine, leucine, and iso-leucine are three essential amino acids that are referred to as the branched chain amino acids (BCAAs, Figure 1). Although they cannot be synthesized by mammals and are solely provided by the diet, they make up approximately 35% of all essential amino acids in mammalian systems (Neinast et al., 2019). These metabolites are extremely sensitive to the actions of insulin and are intimately linked to the onset of insulin resistance. High circulating BCAAs are a clinical sign which is strongly associated with multiple indices of insulin resistance (Yoon, 2016; Zhao et al., 2016), and are evident during obesity, T2DM, and NAFLD. Under normal physiological conditions, BCAAs are utilized for protein synthesis or oxidized for energy (Neinast et al., 2019). This oxidation that occurs in the tissues is regulated by insulin, and is impaired when insulin resistance is present. The dysfunction of these catabolic pathways is thought to be the contributing factor for increased circulating levels during insulin resistance (Wang et al., 2019).

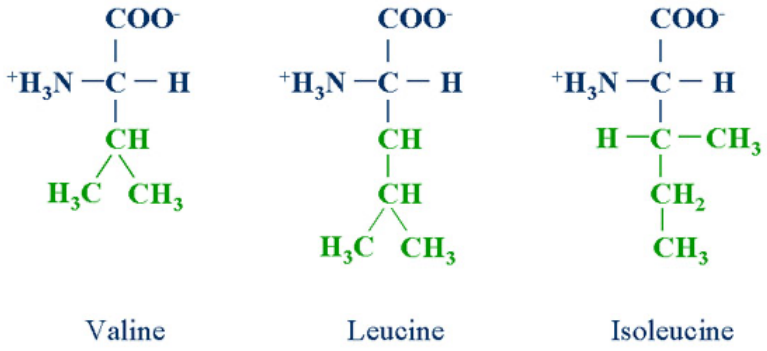

Figure 1: Chemical structures of the branched chain amino acids Valine, Leucine, and Isoleucine, Source: (Proteomics, n.d.)

Tissue BCAA Degradation Pathways

Muscle is the dominant tissue that catabolizes BCAAs. Adipose, liver, kidney, heart, and brain tissue are other contributors to BCAA degradation (Holeček, 2018). The first step in the catabolism of BCAAs is catalyzed by the enzyme branched-chain-amino-acid aminotransferase (BCAT). In the cytosol, BCAT trans-aminates the BCAAs. Alpha-ketoglutarate is the amino group acceptor and this reaction forms the corresponding branched chain keto-acids (BCKAs) and glutamate as products. The second step of BCAA catabolism occurs within the inner membrane of the mitochondria. The activated branched chain keto acid dehydrogenase (BCKDH) complex releases CO_2, reduces NAD+ to NADH, adds a Co-A molecule to the branched chain keto acid, and this can then be used to replenish TCA cycle intermediates and form ketones (Neinast et al., 2019). Leucine degradation yields ketogenic products, valine serves as gluconeogenic substrates, and isoleucine can produce both ketogenic and gluconeogenic products (Figure 2).

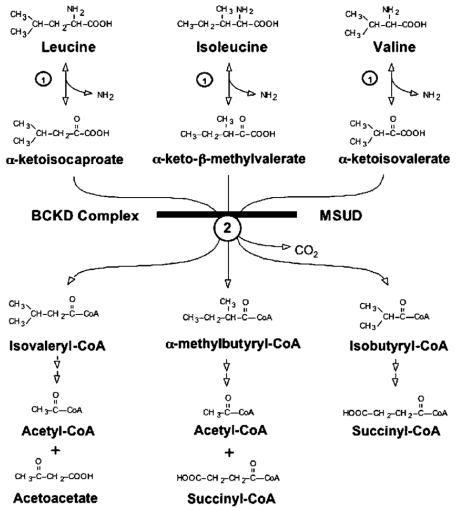

Figure 2: Specific degradation pathways for each of the BCAAs. Source: (Chuang et al., 2006)

Due to the responsiveness of the BCAA degradation networks to insulin, it is clear that that insulin resistance would impair the efficiency of this pathway leading to an accumulation of BCAA degradation substrates and intermediates. Several studies have linked obesity and high lipid consumption with decreased expression of the BCAA catabolism enzymes BCAT and BCKDH (Estrada-Alcalde et al., 2017; Lackey et al., 2013), highlighting the BCAA degradation impairment that occurs during obesity. Additionally, increasing expression of these enzymes is one of the effects of a popular drug class Thiazolidinediones (TZDs). These drugs are prescribed to improve insulin sensitivity. TZDs mechanism of action is they activate peroxisome proliferator activated receptor-gamma (PPARγ), which regulates the gene expression of proteins associated with glucose, lipid, and protein homeostasis (Eggleton & Jialal, 2021). Blanchard et al. provides evidence that activation of PPARγ rescues BCAA oxidation levels and contributes to reducing circulating BCAA levels in an obese mouse model system (2018).

Normal Adipose Tissue Function and Physiology in White and Brown Adipose Tissue

Homeostatic regulation of energy via the utilization and supplementation of circulating metabolites is the goal of nutrient metabolism. Many tissues, such as skeletal and cardiac muscle, liver, and adipose use specialized mechanisms and processes to achieve this goal. Adipose tissue, the focus of this thesis, both stores and supplies energy to the body in the form of lipids.

Adipose tissue is found in localized areas of the body, referred to as adipose depots. Preferential storage of lipids in these depots can be used to estimate metabolic health and the propensity to develop diseases in future (Haczeyni et al., 2018). Two

types of adipose depots determine this: visceral and subcutaneous. Visceral depots are found within the abdominal cavity and in close proximity to the gastrointestinal tract and subcutaneous depots are localized under the skin. Comparing the size of the visceral depots to subcutaneous depots can serve as predictors of overall metabolic health. Large visceral depots indicate a metabolically unhealthy individual with a higher risk of developing insulin resistance and heart disease (Klein, 2004). The mechanisms by which lipids are preferentially stored in visceral or subcutaneous depots remain unknown.

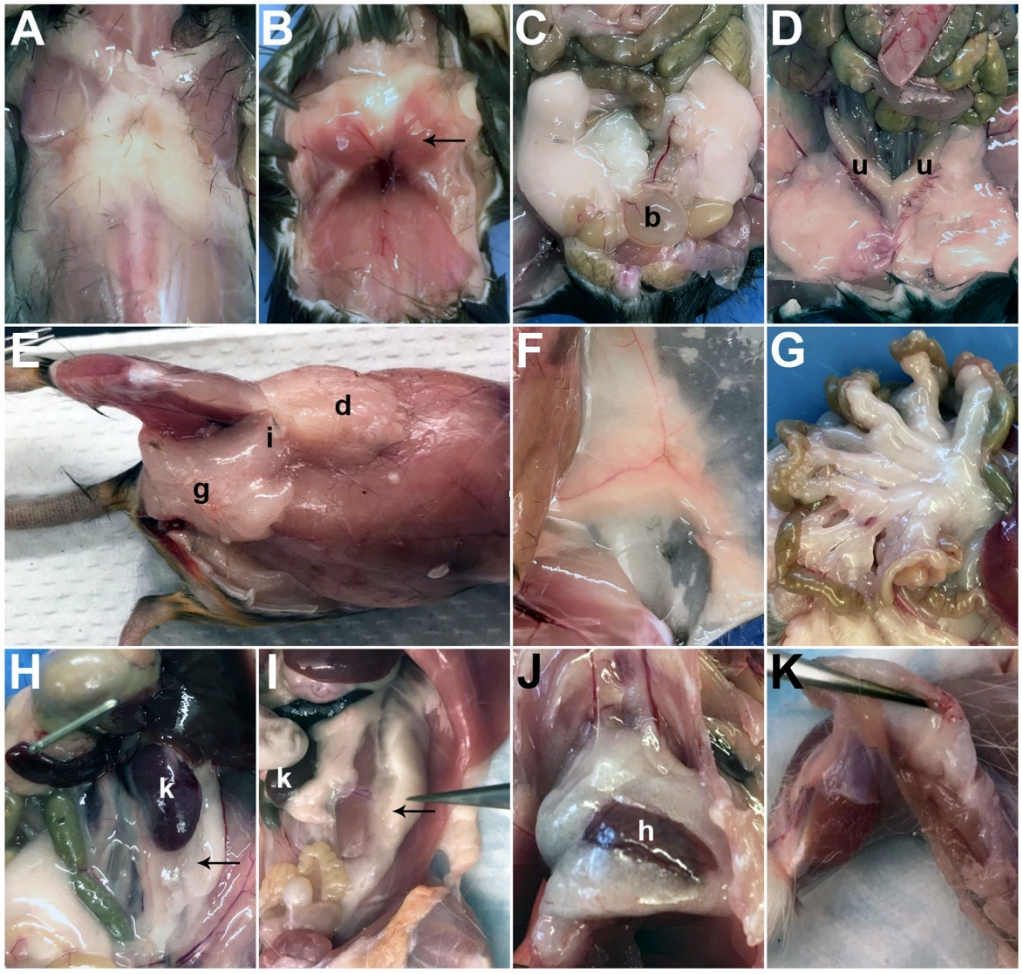

Figure 3: Various murine adipose depots. Source: (Bagchi & MacDougald, 2019)

Adipose tissue is comprised primarily of adipose cells (adipocytes), but it is important to note that other cell types contribute to adipose tissue development and function as well. Among these cells are: macrophages, lymphocytes, vascular cells, and pre-adipocytes (Ouchi et al., 2011). All adipocytes have the general function of lipid storage and mobilization, but the end goal and physical characteristics can differ. The two general types of adipose tissue, brown (BAT) and white (WAT), differ in both physical characteristics and metabolic functions.

WAT is the most abundant adipocyte type found in the body. 90% of WAT cell volume is comprised of a unilocular lipid droplet (Saely et al., 2012). The lipid droplet is considered an organelle and protects the cell and peripheral tissues from lipotoxicity by storing excess lipids within it (Luo & Liu, 2016). These cells are spherical and their size is dependent on the amount of lipids store. As excess nutrients are taken up, white adipocytes expand to accommodate more lipid storage. During fasting or energy deficiency, when lipid stores are utilized, the cells shrink moderately. This plasticity during feeding and fasting is one of the specialized mechanisms by which WAT maintains energy homeostasis in the body.

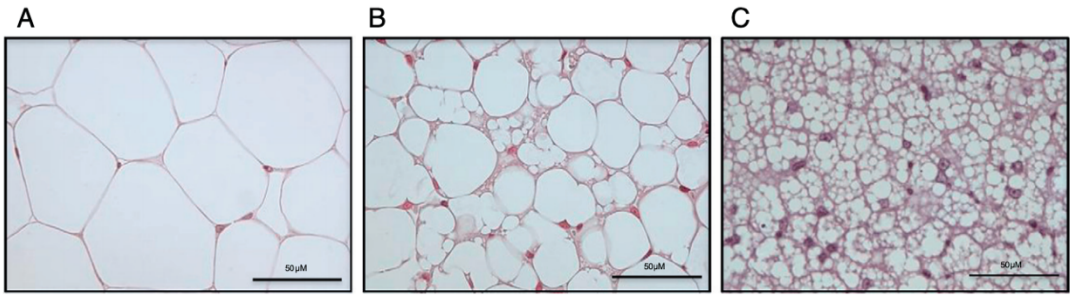

Figure 4: Histological examples of white (A), beige (B), and brown (C) adipose tissue. Source: (Keipert & Jastroch, 2014)

Brown adipocytes are highly specialized cells whose main role is thermogenesis. These adipocytes form many, small intracellular lipid droplets and have numerous mitochondria, which give the tissue its characteristic brown color. Mitochondria in brown adipocytes are specialized for non-shivering thermogenesis and can defer the end product of oxidative phosphorylation from energy to heat production during cold environmental conditions. This is achieved by the use of uncoupling protein-1 (UCP-1), found at the end of the electron transport chain. Activation of this protein allows for the oxidation of fatty acids to generate heat (Saely et al., 2012). The amount of BAT in an organism is very little compared to WAT, and depends on the ambient environment of the organism. Animals living in a cold climate produce more BAT, as thermogenesis is an important part of their survival. Animals in warm climates have BAT that resembles WAT, with large lipid droplets and adipocytes that cater more towards lipid storage.

A recent advancement in the understanding of adipose has revealed a third type of tissue called beige adipose tissue. As the name implies, beige tissue is a hybrid of white and brown. During cold challenges, “beigeing” can occur, where this tissue resembles BAT and even expresses UCP-1, the BAT specific thermogenesis protein. However, during normal conditions it looks characteristically similar to WAT. Beige tissue appears to only be found in certain adipose depots, such as the inguinal and scapular areas of the body (Sanchez-Gurmaches et al., 2016). It is a current area of study as to where these cells originate. If they have BAT origins that would explain the similarities. This topic, however, is more complex than it seems. Research is being

conducted to further understand this tissue, its origins, and how it can be utilized as a potential target area for the treatment of obesity and type II diabetes.

Adipose as a Endocrine Organ

Originally thought of simply as a storage organ, adipose tissue has been revealed to be an important endocrine organ releasing factors that both prevent and progress metabolic diseases. These adipose specific endocrine factors are referred to as adipokines. Most adipokines are pro-inflammatory and have been linked to the advancement of systemic metabolic dysfunction beginning with adipose tissue (Ouchi et al., 2011). One of these adipokines is leptin, an appetite hormone linked to obesity and insulin resistance. Leptin is the hormone that communicates the levels of energy storage in adipose tissue to the hypothalamus of the brain. High leptin release serves as a signal that energy stores are sufficient and the system can reduce feeding. During times of starvation or fasting, leptin levels fall and allow normal feeding and the replenishment of lipid stores. Clinical deficiency of leptin causes hyperphagia (overeating) and obesity, and is precisely the mechanism behind the *ob/ob* mouse which is popularly used as a model of obesity. During normal obesity, leptin levels are chronically high in response to excess nutrient uptake. Eventually, leptin resistance will develop and will no longer efficiently signal the reduction of feed intake (Kelesidis et al., 2010).

It is recognized that metabolic dysfunction is progressed by chronic inflammatory states. Adipose releases a number of inflammatory adipokines, including tumor necrosis factor (TNF) and interleukin-6 (IL6). When adipocytes expand to a critical size, they release inflammatory adipokines and recruit macrophages, which

contribute to this inflammatory response by producing TNF. Obese individuals with high adiposity present higher levels of TNF and IL-6 and these levels are reduced with weight loss (Ouchi et al., 2011).

An anti-inflammatory and insulin sensitizing cytokine produced by adipose is adiponectin. It impacts liver, muscle, adipose, and vascular tissue and is a potent target for insulin resistance and obesity treatment because of its beneficial impacts. Adiponectin signaling pathways positively impact insulin signaling and fatty acid oxidation. In *ob/ob* mice, over expression of adiponectin not only rescued dietary induced insulin resistance, but also reduced inflammation by decreasing macrophage presence and TNF levels in the adipose tissue (Kim et al., 2007). It has also been reported that the 3T3L1 pre-adipocyte cell line releases high amounts of adiponectin, indicating a positive correlation between adipocyte differentiation and adiponectin (Achari & Jain, 2017).

Factors Influencing Adipose Expansion and Differentiation

Adipose expansion is the process of increasing the size of adipose tissue. This is achieved either by increasing the size of the existing adipocytes (hypertrophy) or increasing the number of new adipocytes (hyperplasia). Initially, as more excess lipids are taken up or formed, adipocytes will expand the intracellular lipid droplets to accommodate. However, after the cells reach critical size and can no longer expand, they begin releasing inflammatory cytokines like interleukin-6 (IL-6) and tumor necrosis factor alpha (TNF-alpha) (Choe et al., 2016). Other hormone profiles are altered during hypertrophy, such as decreased adiponectin and increased leptin release. As adiponectin and leptin are hormones related to insulin sensitivity, hypertrophic

adipocytes have a higher propensity to develop insulin resistance. Also released are differentiation cytokines that signal for pre-adipocytes to begin differentiation and maturation.

Adipocyte Differentiation

Each adipose depot has its respective pool of pre-adipocyte cells present. When adipocytes form from mesenchymal precursor cells, they undergo differentiation. Differentiation is the process by which the cell changes its gene expression to display the adipocyte phenotype. This process is regulated by transcription factors such as C/EBPα and PPARγ, which express early in the differentiation process and maintain expression through a positive feedback loop to preserve the adipocyte phenotype (Siersbaek et al., 2010).

It was previously accepted that due to the distinct differences in brown and white adipocytes, they would have different cellular origins. This, however, has been proven to be more complex. Studies have shown that there is not a single origin for BAT or WAT, but multiple precursor cells exist for white and brown tissue (Sanchez-Gurmaches et al., 2016). There is still much to be studied and understood in the area of adipocyte differentiation, cell origin, and the process and determining factors for adipocyte commitment.

Adipose Tissue and Lipid Metabolism

In any metabolic process there are two pathways: synthesis (anabolism) and degradation (catabolism). In adipocyte lipid metabolism, the anabolic and catabolic pathways are lipogenesis and lipolysis, respectively. Lipid sources include endogenous

de novo lipids and dietary lipids from food intake. *De novo* lipids can be synthesized using acetyl co-A derived from glycolysis or from fatty acid oxidation. Lipogenesis is highly regulated by many factors including hormones, gene expression, and nutrition (Kersten, 2001). These newly formed lipids are stored in the lipid droplets of the cell, which protect the adipocyte from lipo-toxicity. The lipogenesis pathway is favored during times of nutrient intake and abundance. Conversely, during fasting or starvation fatty acids are released from the lipid droplets to provide energy to peripheral tissues. This process is lipolysis (Figure 5). The adipocyte contains several lipases that cleave fatty acids from the glycerol back bone. This process converts a triglyceride to a diacylglycerol, and further to a monoacylglycerol. The fatty acids and glycerol released by lipolysis are utilized by the adipocyte or transported through the blood to provide energy to other tissues and organs.

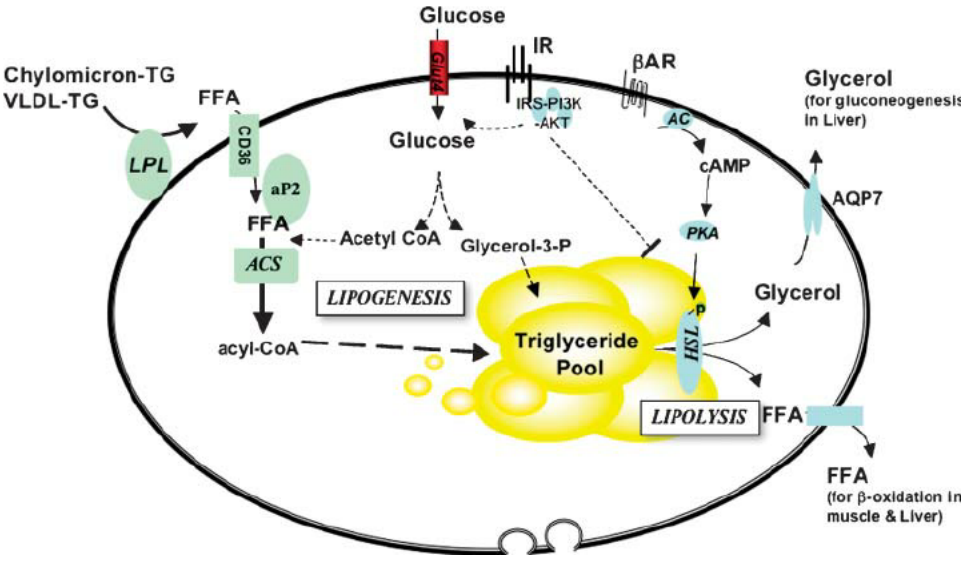

Figure 5: Overview of lipid metabolism in adipocytes. Source: (Sethi, 2007)

Evidence of BCAAs and Adipose Tissue Expansion and Differentiation

Adipocyte differentiation is fueled by BCAA catabolism. Green, et al. reports 30% of the acetyl Co-A pool used in lipogenesis is derived from BCAA catabolism (Green et al., 2016). Estrada-Alcade, et al. demonstrated that BCAA deprivation inhibits cell differentiation and lipid accumulation in maturing adipocytes while BCAA supplemetation significantly increases lipid formation (Estrada-Alcalde, Isabela et al., 2016). In the same study, using isotope tracers, incorporation of BCAAs into maturing adipocytes was quantified. During the later stages of differentiation, there are significant increases in the incoportation of BCAA (especially Leucine) degradation products into lipid and protein synthesis.

PPARγ, the differentiation transcprition factor that promotes expression of adipocyte characteristics, also increases BCAA degradation. PPARγ agonists are commonly used drugs to combat insulin resistance. One such drug, Rosiglitazone, when admistered to rats on a HF diet, restored down-regulated BCAA degradation enzymes and lowered circulating BCAA levels (Blanchard et al., 2018). One question that requires more study is if increasing BCAA levels in a normal animal can "reverse" activate PPARγ, and possibly induce adipocyte differentiation.

Evidence of BCAAs and Adipose Tissue Lipolysis

The process of lipolysis has many molecular regulators such as hormones, cytokines, and enzymes. It is known that BCAAs stimulate mammalian target of rapamycin (mTOR), a kinase that is involved in numerous homeostatic and metabolic networks (Yoon, 2016). In adipose, mTOR activation increases fatty acid synthesis, adipocyte differentiation, and lipogenesis (Soliman, 2011). More recently, the impact

of mTOR activity on lipolysis has been discussed. Soliman (2010) demonstrated that treatment of 3T3-L1 adipocytes with rapamycin, a mTOR inhibitor, increased lipolysis. Therefore, these results demonstrate that mTOR activation inhibits lipolysis. The conundrum, however, is that although BCAAs have been shown to activate mTOR, which inhibits lipolysis, BCAAs have also been shown to increase lipolysis themselves.

Heng et al. (2020) has shown increased levels of lipolysis and higher expression of lipolytic proteins when weanling piglets were fed a high-BCAA diet. Interestingly, these same changes in lipid metabolism were also seen in piglets fed low-BCAAs diets in the same study. The mechanism by which BCAAs increase lipolysis is described by this paper as BCAAs modifying m^6A RNA methylation. In a high-fat diet condition, mice supplemented with BCAAs showed increased lipolytic rates despite simultaneous treatment with insulin (Zhang et al., 2016). These studies provide evidence that BCAAs impact lipolysis, however a mechanism remains to be elucidated, as well as determining if this impact on lipolysis is beneficial or harmful for normal and insulin resistant physiology,

Adipose Tissue, BCAA degradation, and Mitochondrial Function

The association between adipose tissue, BCAA degradation, and mitochondrial function in relation to metabolic diseases is a large area of study. Mitochondria play critical, adipocyte specific roles in adipose tissue functions (Figure 6) including adipocyte differentiation, lipid metabolism, thermogenesis, and insulin sensitivity. However, dysfunction of mitochondria during obesity and IR can impact the mitochondria's ability to regulate and aid in these pathways that maintain normal adipocyte function. This can stem from an accumulation of reactive oxygen species

(ROS) during chronic, mitochondrial oxidative stress (Lee et al., 2019), and accumulated ROS can further induce IR.

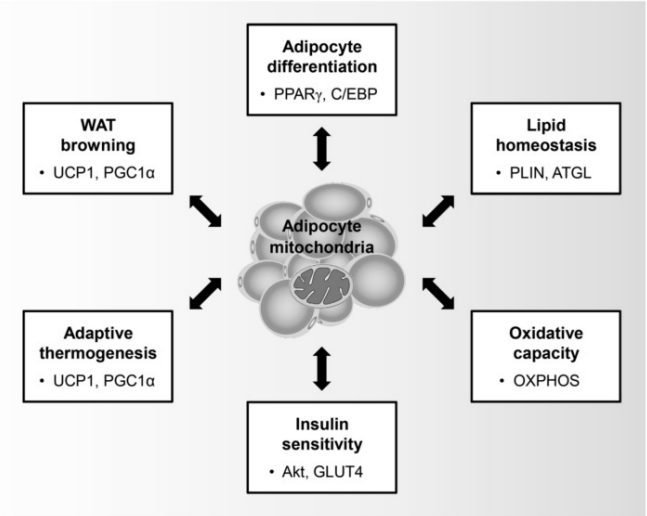

Figure 6: Specific roles of mitochondria in adipose tissue. Source: (Lee et al., 2019)

As previously mentioned, BCAAs are susceptible to the actions of insulin and are also impacted during insulin resistant metabolic states, specifically the degradation of BCAAs. BCAA degradation products can also replenish the TCA cycle. Adipose tissue is recognized as an organ that is responsible for the catabolism of considerable amounts of BCAAs and is involved in the whole-body homeostatic regulation of circulating amino acids (Herman et al., 2010). Since BCAA metabolism occurs partly in the mitochondria and further fuels mitochondrial pathways, impairment of either BCAA catabolism or mitochondrial function will inevitably impact the other.

Chapter 3: Experimental Design and Methods

Animals

All animal protocols were approved by the University of Maryland Institutional Care and Use committee. Mice were housed at 22°C with a 12-h light-dark schedule, and given feed and water ad libitum. 6-8 week old C57-BL6N male mice (Jackson Laboratory) were kept on four specialized custom diets (Research Diets, Inc., see Table 1) for 12-34 weeks: low-fat (LF, 10% fat, D12450J), low-fat supplemented with BCAAs (LB, 10% fat, 150% BCAAs, D19050804), high-fat (HF, 60% fat, D12492), and high-fat supplemented with BCAAs (HB, 55% fat, 150% BCAAs, D19121607). Cages were stocked with 3-5 mice each, and all mice within a cage were on the same custom diet. Body weights of each mouse and the feed intake of the cages were measured weekly. Mice were randomized into fed and fasted (~16 hours overnight) groups, euthanized under isoflurane anesthesia, and adipose and blood were collected. Part of the tissues were used fresh, fixed in formalin for histology, or flash frozen in liquid nitrogen and stored at -80°C for further analysis. Serum was isolated by centrifuging the clotted blood at 3,000rpm for 10 minutes and taking the supernatant. Serum stored at -80°C for further analysis.

Table 1

Custom Mouse Diet Compositions

	Low Fat (LF)		**Low Fat w/ BCAA (LB)**		**High Fat (HF)**		**High Fat w/ BCAA (HB)**	
Product #	D12450J		D19050804		D12492		D19121607	
% kcal Protein	20		25 (150% BCAA)		20		25 (150% BCAA)	
% kcal Carbohydrate	70		65		20		20	
% kcal Fat	10		10		60		55	
Ingredients	grams	kcal	grams	kcal	grams	kcal	grams	kcal
Casein	200	800	200	800	200	800	200	800
L-Cystine	3	12	3	12	3	12	3	12
L-Isoleucine	0	0	**11.46**	46	0	0	**11.46**	46
L-Leucine	0	0	**23.97**	96	0	0	**23.97**	96
L-Valine	0	0	**14.11**	56	0	0	**14.11**	56
Maltodextrin 10	125	500	125	500	125	500	125	500
Corn Starch	506.2	2025	456.66	1827	0	0	0	0
Sucrose	68.8	275	68.8	275	68.8	275	68.8	275
Cellulose, BW200	50	0	50	0	50	0	50	0
Soybean Oil	25	225	25	225	25	225	25	225
Lard	20	180	20	180	245	2205	223	2007
Mineral Mix S10026	10	0	10	0	10	0	10	0
DiCalcium Phosphate	13	0	13	0	13	0	13	0
Calcium Carbonate	5.5	0	5.5	0	5.5	0	5.5	0
Potassium Citrate, 1 H20	16.5	0	16.5	0	16.5	0	16.5	0
Vitamin Mix V10001	10	40	10	40	10	40	10	40
Choline Bitartrate	2	0	2	0	2	0	2	0
FD&C Yellow Dye #5	0.04	0	0.05	0	0	0	0.05	0
FD&C Red Dye #40	0	0	0	0	0	0	0	0
FD&C Blue Dye #1	0.01	0	0	0	0.05	0	0	0
Totals	1055.5	4057	1055.5	4057	773.85	4057	801.39	4057
kcal/g	3.85		3.85		5.24		5.06	

Note. Composition of the specialized diets on which mice were reared for up to 34 weeks. Purchased from Research Diets, Inc.

In-Vitro Lipolysis Assay

As an index of adipose lipolysis, three *in vitro* lipolysis assays utilizing adipose tissue explants were performed. The first assay utilized mice on diets for 34 (LF and LB) or 24 (HF and HB) weeks. The media consisted of Dulbecco's modified eagle medium (DMEM, Sigma-Aldrich, D6046), 10µM isoproterenol (Caymen Chemicals), 5µM Triacsin-C (Caymen Chemicals), and 2% FA-free bovine serum albumin (BSA) (See Table 2 for media formulation per treatment). To stimulate the tissue, isoproterenol (ISP), a catecholamine that induces lipolysis by serving as a beta-adrenergic receptor agonist that increases levels of cAMP (Szymanski & Singh, 2021), was added to the media. The addition of Triacsin-C was to prevent re-esterification of released fatty acids. A 10mM stock of isoproterenol and 5mM stock of Triacsin C were made in DMSO and stored at -20°C. Media was made fresh before each experiment. 200µL of each media was added to a 96-well plate which was pre-warmed at 37°C. Fresh perigonadal WAT was cut into ~50mg pieces and placed in the plate containing the pre-warmed media. The plate was pre-incubated for 1 hour at 37°C and 5% CO_2, then the adipose was transferred to new wells containing 200µL of fresh, identical media and incubated in the same conditions for another hour. The adipose tissue and media were stored separately at -80°C for further analysis.

The second lipolysis assay used 12 week dietary treated animals and increasing concentrations of BCAAs. For this experiment, a custom media devoid of BCAAs was necessary so we could add the desired concentrations (Table 3). Media was premade with BCAA concentrations of 500µM and 1mM and stored at -20°C. On the day of the experiment, media was thawed and 200µL was added to a 96-well plate and pre-

warmed at 37°C. ~30mg tissue explants were added to a pre-cooled plate containing DPBS until all explants were cut and weighed. Then they were transferred to the pre-warmed plate and pre-incubated for 2 hours at 37°C and 5% CO_2. After pre-incubation, explants were moved to a new well containing 200µL of fresh, identical media and incubated again for 1 hour. To rinse excess BSA in the media from the explants, they were washed in DPBS before storing. Adipose and media were stored at -80°C for further analysis.

For the final lipolysis assay, normal chow-fed male mice were used. The same custom media (Table 3) was used, but with BCAA concentrations of 50µM, 500µM, 1mM, and 2.5mM. This media also was used with and without 2.5µM isoproterenol. Before the experiment, the media was thawed and divided into two aliquots per BCAA concentration. The appropriate amount of 10mM isoproterenol stock was added to one aliquot for a final concentration of 2.5µM isoproterenol. 200µL of each media was loaded into a 96-well plate and pre-warmed at 37°C. ~30mg of perigonadal WAT explants were cut and sliced on a chilled ceramic tile on ice using a scalpel. This was to maximize the surface area of the tissue in contact with the media. Then the slices were transferred to a chilled plate containing DPBS. Once all explants were cut, weighed, and sliced, they were transferred to their respective wells in the pre-warmed plate. Pre-incubation at 37°C and 5% CO_2 occurred for 1 hr. The slices were carefully transferred to a new well containing 200µL of fresh, identical media and incubated for 2 more hours. After incubation, the tissue was washed of excess BSA by washing with DPBS prior to storage. Media and tissue explants were stored at -80°C for further analysis.

Table 2

Lipolysis Assay Media composition by Treatment

Treatment	Media
Basal	DMEM with 2% BSA
Isoproterenol (ISP)	DMEM with 2% BSA, 10μM ISP, and 5μM Triacsin-C

Note. Media compositions per treatment for lipolysis assay using mice on custom diets for 34 and 24 weeks. DMEM-Dulbecco's modified eagle medium, BSA- bovine serum albumin

Table 3

Custom Adipose Tissue Explant Media

DPBS (Gibco, 14040-117)	368mL
NEAAs (100x, Gibco 1140-050)	4mL
EAAs (25x, see Table 4)	16mL
L-Glutamine (200mM, Gibco 25030-081)	2mL
MEM Vitamix (100x, Gibco 11120-052)	4mL
FA-Free BSA (Thermo-Fisher)	8g
BCAA Stock (Table 5)	Varies

Note. Recipe for 400mL of custom media for adipose tissue explants. After all ingredients except for the BCAA stock was added and dissolved, media was aliquoted for BCAA concentrations and the proper amount of BCAA stock was added (Table 5). Then the media was brought to a pH of 7.4 at 37°C, filtered, aliquoted, and stored at -20°C. DPBS-Dulbecco's phosphate-buffered saline, NEAA- non-essential amino acids, EAA- essential amino acids, MEM- minimum essential medium

Table 4

Non-Essential Amino Acid (NEAA) 25x Stock Composition

Amino Acid	Weight (g)	Concentration in 25x stock (mM)	Concentration in 400mL media (mM)
L-Arginine (Fisher, BP373)	0.063	18.08	0.7232
L-Cystine (Sigma, C7602)	0.006	1.24	0.0496
L-Histidine (Sigma, H8125)	0.0209	4.985	0.1994
L-Lysine (Sigma, L5626)	0.036	9.85	0.394
L-Methionine (Sigma, M9625)	0.007	2.34	0.0936
L-Phenylalanine (Sigma, P2126)	0.0165	4.99	0.1996
L-Threonine (Sigma, T8625)	0.023	9.65	0.386
L-Tryptophan (Sigma, T0254)	0.005	1.224	0.0489
L-Tyrosine (Sigma, T3754)	0.018	4.967	0.1986

Note. Recipe for 25x NEAA stock for custom adipose tissue explant media (Table 3). Amino acids were weighed and dissolved in 20mL of 0.1N HCl, and stirred at 65°C for approximately one hour or until completely dissolved. The stock was aliquoted and stored at -20°C.

Table 5

BCAA Stock Composition

BCAA	Weight (mg)	Concentration in 50mL
L-Leucine	660.1	100.65mM
L-Isoleucine	408	62.21mM
L-Valine	586	100.2mM

Note. BCAA stock solution used to make custom adipose explant incubation media. BCAAs were weighed, added to 50mL of 0.1N HCl, and stirred until dissolved. The stock solution was aliquoted and stored at -20°C.

Analysis of Non-Esterified Fatty Acids (NEFA)

NEFA assay kits were purchased from Wako Diagnostics. A standard curve was constructed using 1, 0.75, 0.5, 0.25, 0.125, 0.0625, 0.031, and 0 mM of 0leic acid (Wako Diagnostics). 5µL of standard and sample (lipolysis assay media or serum) was loaded per well, then 200µL of Reagent A was added. The plate was incubated at 37°C for 5 minutes and read at a 550nM. Then 100µL of Reagent B was added to each well and incubated another 5 minutes at 37°C. The plate was read again at 550nM. To obtain the final concentrations, the first reading absorbance values were subtracted from the second absorbance values. This corrected absorbance was used to construct the standard curve and determine the concentration of NEFA in the sample.

Analysis of Glycerol in Lipolysis Incubation Media

To measure free glycerol in the lipolysis assay media, glycerol reagent from Sigma-Aldrich was used. A standard curve was constructed using glycerol diluted in the base media used in the lipolysis assay (DMEM). 5µL of standard and sample were loaded into a 96-well plate, and 200 µL of glycerol reagent was added. The plate was incubated at 37°C for 5 minutes an read at 540nM. Using the constructed standard curve, the concentration of free glycerol in the sample was calculated.

Western Blot Analysis of Adipose Tissue Proteins

To extract protein from the adipose tissue, 200µL of cold 1x RIPA (Table 6) with protease and phosphatase inhibitors (Fisher Scientific) was added to a tube containing frozen adipose tissue (~100mg WAT, ~10mg BAT) and zirconium oxide beads. The tissue was lysed using a bead mill homogenizer (VWR) on speed 5 for 30

seconds, allowed to rest on ice for 30 seconds, and repeated twice more. Once homogenized, the lysate was incubated on ice for one hour. To separate the fat from the protein lysate, the samples were spun at 20,000g and 4°C for 30 minutes. 125µL of the protein lysate was then carefully removed from under the fat layer using a gel-loading pipette tip. A BCA assay (Thermofisher) was used to determine the protein concentration.

The protein was diluted to a concentration of 2µg/µL using water, and appropriate amounts of running buffer (4:1 Bolt 4x, Thermofisher Scientific, and ß-mercaptoethanol, Sigma-Aldrich) were added to each sample. The samples were heated at 95°C for 5 minutes, aliquoted, and stored at -80°C until use. Premade gels (Invitrogen) were used and the samples were run using a 1x SDS MES running buffer (Fisher Scientific). The gel was transferred to a PVDF membrane (Fisher Scientific), blocked in 5% milk and incubated in the primary antibody (1:1000 dilution in 3%BSA, 0.02% sodium azide, 1x TBS Tween) overnight at 4°C. The following day, the membrane was incubated in the secondary antibody (1:10,000 dilution, in 5% milk and 1x TBS Tween) for one hour at room temperature. The membrane was washed with 1X TBS-Tween three times for five minutes each between each step from blocking to imaging. To image, Pico West Plus and Lumigen were used. Antibodies used: COXIV (Cell Signaling, #11967), Beta-Actin (Cell-Signaling, #3700), OXPHOS antibody cocktail (Abcam, ab110413), anti-mouse secondary (Cell Signaling, #7076).

Table 6

Recipe for 1x RIPA Lysis Buffer

25mM Tris (pH 8.0)	1.51g (in 400mL of diH_2O)
150mM NaCl	4.38g
1% NA Deoxycholate	5g
1% Triton X-100	5mL
5mM EDTA	0.93g
0.1% SDS	0.5g

Note. Dissolve Tris base in 400mL diH_2O, adjust pH to 8.0 using HCl, add remaining compounds, and adjust the final volume to 500mL using diH_2O.

Measurement of Circulating Biomarkers

To measure changes in serum hormone concentrations, serum analysis was conducted. ELISA assay kits were purchased from Crystal Chem for mouse insulin (90080), adiponectin (80569), and leptin (90030). No changes to the manufacturers guidelines were made.

Gene Expression Profiles

For WAT, ~100mg frozen tissue was added to an RNAse-DNAse free tube containing ceramic beads. 1mL of Trizol Reaget (Fisher Scientific) was added and the tissue was homogenized using a VWR Mini-Bead mill at speed 5 for 30 seconds. Samples are incubated at room temperature for 5 minutes to allow complete dissociation of nucleoproteins. The homogenate is then centrifuged at 12,000g for 10 minutes at 4°C. Avoiding the disturbance of the fat layer, 600µL of the RNA solution is removed and placed in a fresh tube. Then, 200µL of chloroform is added to each tube, shaken vigorously for 15 seconds, and incubated at room temperature for 3 minutes. To separate the layers, the tubes are centrifuged at 12,000g for 15 minutes at 4°C . 300µL of the upper, colorless layer is removed and placed in a fresh tube. An equal amount of 95-100% ethanol is added and mixed by pipetting. Then RNA isolation is carried out using the Zymo Direct-zol RNA Mini Prep kit (Genesee Scientific, 11-330). For BAT, ~100mg frozen tissue is added to an RNAse-DNAse free tube containing ceramic beads. 600µL of Trizol reagent is added and the tissue is homogenized using a VWR Mini-Bead Mill on speed 5 for 30 seconds. The tubes are centrifuged at 13,500rpm for 5 minutes at 4°C. 350µL of supernatant is transferred to a fresh tube, and an equal volume of 100% ethanol is added and mixed by pipetting.

Then RNA isolation is carried out using the Zymo Direct-zol RNA Mini Prep kit (Genesee Scientific, 11-330).

RNA concentration and quality are measured using a Biotek Take3 plate and Cytation5 Imager. The RNA concentration is adjusted using RNA-ase/DNA-ase free water, and 1µg RNA is added to iScript Reverse Transcriptase mix. cDNA is synthesized, diluted to a total volume of 50µL per sample. For qPCR, 25ng of template cDNA, 500nM of forward and reverse primer, and EvaGreenER buffer are used. Results were analyzed using the methods described by Livak & Schmittgen (2001). qPCR primer sequences are listed in table 7.

Adipose Histology

A small piece of fresh adipose tissue was carefully cut from the middle of the depot, avoiding jagged edges when cutting. The tissue was fixed in 10% formalin at room temperature overnight. The following day tissue was washed three times in 70% ethanol to remove excess formalin and stored in 70% ethanol at 4°C until pickup. Embedding in paraffin wax, slicing, H&E staining, and slide imaging were done by Histoserv, Inc. Representative images were taken of each slide and cropped to be identical in size.

Table 7

Oligonucleotide sequences for qPCR primers

Gene	Forward	Reverse
Bcat2	5'-CAGCCACACTAGGACAGGTCT-3'	5'-CAGCCTTGTTATTCCACTCCAC-3'
Bckdk	5'-ACATCAGCCACCGATACACAC-3'	5'-GAGGCGAACTGAGGGCTTC-3'
Cyclo	5'-GGAGATGGCACAGGAGGAA-3'	5'-GCCCGTAGTGCTTCAGCTT-3'
Pgc1α	5'-AGACAAATGTGCTTCCAAAAAGAA-3'	5'-GAAGAGATAAAGTTGTTGGTTTGGC-3'
PparY	5'-CTCTGGGAGATTCTCCTGTTGA-3'	5'-GGTGGGCCAGAATGGCATCT-3'
Ucp1	5'-CACCTTCCCGCTGGACACT-3'	5'-CCCTAGGACACCTTTATACCTAATGG-3'

GC-MS Metabolomics

Frozen adipose tissue (~100mg for WAT, ~10mg for BAT) was added to a tube containing ^{13}C labeled stable isotope standards (Tables 8, 9, and 10), water, 2:1 chloroform: methanol, and zirconium oxide beads. The tissue was homogenized for 30 seconds using a mini bead mill (VWR) on speed 5. A one hour extraction was performed on ice, vigorously shaking the samples every 10 minutes. To separate the layers, the samples were spun at 3,000rpm for 5 minutes at 4°C. The upper aqueous layer was removed and dried under nitrogen. To generate oximes, 2% methoxyamine hydrochloride in pyridine was added and the samples microwaved at 350W for 90 seconds. Then the metabolites were converted to TBDMS derivatives by heating at 90°C for one hour. Metabolites were run on GC-MS (Agilent): separation was achieved using a HP-5MS UI column and detection used single ion monitoring.

Statistical Analysis

This study utilized a completely randomized design, with the possibility of a cage effect. Mean and standard error of the means (SEM) were calculated for each data set. Significance was calculated using one-way ANOVA or an unpaired t-test. Comparisons were made only between the means of LF vs LB and HF vs HB. Significance was accepted at a p-value less than or equal to 0.05. Graph generation and data analysis were completed using Graphpad Prism.

Table 8

Stable Isotope Labeled Internal Standard for Organic Acids

Organic Acids	Molecular Weight (g/ mol)	Stock Concentration (µM)	Amount (µg) OA in (25 uL) IS
Sodium Pyruvate ($^{13}C_3$)	113.02	257.0	0.726
Sodium Lactate (3,3,3-D3)	115.06	251.2	0.723
Citric Acid (2,2,4,4-D4)	196.15	252.4	1.237
α -Ketoglutaric Acid (3,3,4,4-D4)	150.12	256.8	0.964
Succinic Acid (D6)	124.13	257.4	0.799
Fumaric Acid (D4)	120.1	261.4	0.785
Malic Acid (2,3,3-D3)	137.11	257.1	0.881

Note. Stable isotope labeled internal standard stock concentrations of organic acids which were spiked into each sample for the determination of metabolite concentrations.

Table 9

Stable Isotope Labeled Internal Standard for Amino Acids

Amino Acid	Molecular weight (g/mol)	Stock Concentration (µM)	Amount (µg) AA in IS (25 uL)
L-Alanine ($^{13}C_3$, ^{15}N)	89.09	248	0.55
L-Glycine ($^{13}C_2$, ^{15}N)	75.07	248	0.47
L-Valine ($^{13}C_5$, ^{15}N)	117.1	247	0.72
L-Leucine ($^{13}C_6$, ^{15}N)	131.2	248	0.81
L-Isoleucine ($^{13}C_6$, ^{15}N)	131.2	248	0.81
L-Proline ($^{13}C_5$, ^{15}N)	115.1	245	0.70
L-Methionine ($^{13}C_5$, ^{15}N)	149.2	248	0.93
L-Serine ($^{13}C_3$, ^{15}N)	105.09	247	0.65
L-Threonine ($^{13}C_4$, ^{15}N)	119.1	245	0.73
L-Phenylalanine ($^{13}C_9$, ^{15}N)	165.2	245	1.01
L-Aspartic Acid ($^{13}C_4$, ^{15}N)	133.1	245	0.82
L-Glutamic Acid ($^{13}C_5$, ^{15}N)	147.1	250	0.92
L-Lysine:2HCL ($^{13}C_6$, $^{15}N_2$)	146.2	247	0.90
L-Histidine:HCL:H_2O ($^{13}C_6$, $^{15}N_3$)	155.2	250	0.97
L-Tyrosine ($^{13}C_9$, ^{15}N)	181.2	249	1.13

Note. Stable isotope labeled internal standard stock concentrations of amino acids which were spiked into each sample for the determination of metabolite concentrations.

Table 10

Stable Isotope Labeled Internal Standard for Keto Acids

Keto acids	Molecular weight	Stock Concentration (uM)	Amount (µg) KA in IS (15uL)
α -Ketoisocaproic Acid ($^{13}C_6$)	158.08	52.6	0.125
Sodium 2-Keto-3-Methyl-Pentanoate ($^{13}C_6$)	158.08	50.7	0.12
α -Ketoisovaleric Acid ($^{13}C_5$)	143.06	51	0.109

Note. Stable isotope labeled internal standard stock concentrations of keto acids which were spiked into each sample for the determination of metabolite concentrations..

Chapter 4: Results

Objective 1:The Impact of BCAAS on Adipose Tissue Morphology and Development

First, to study the impact of BCAA supplementation on adipose tissue morphology and development, we began by characterizing the phenotypes of the mice reared on the four different diets. After 12 weeks on the custome diets, the low-fat BCAA supplemented group (LB) had significantly higher body weights compared to their control counterparts (Figure 7A). There was no difference in body weights between LF and LB after 34 weeks on diet. High-fat (HF) fed animals showed no differences from their BCAA supplemented counterparts (HB) in body weights after 12 or 24 weeks on the custom diets (Figure 7B).

Perigonadal adipose tissue weights were significantly higher in the 12 week BCAA supplemented group, LB compared to LF (Figure 7C). Conversely, after 34 weeks of BCAA supplementation, fasted perigonadal adipose weights in the LB mice were lower than their LF counterparts (Figure 7C). However, 24 weeks of BCAA supplementation on a high-fat background resulted in significantly higher perigonadal adipose weights after fasting, compared to their HF counterparts.

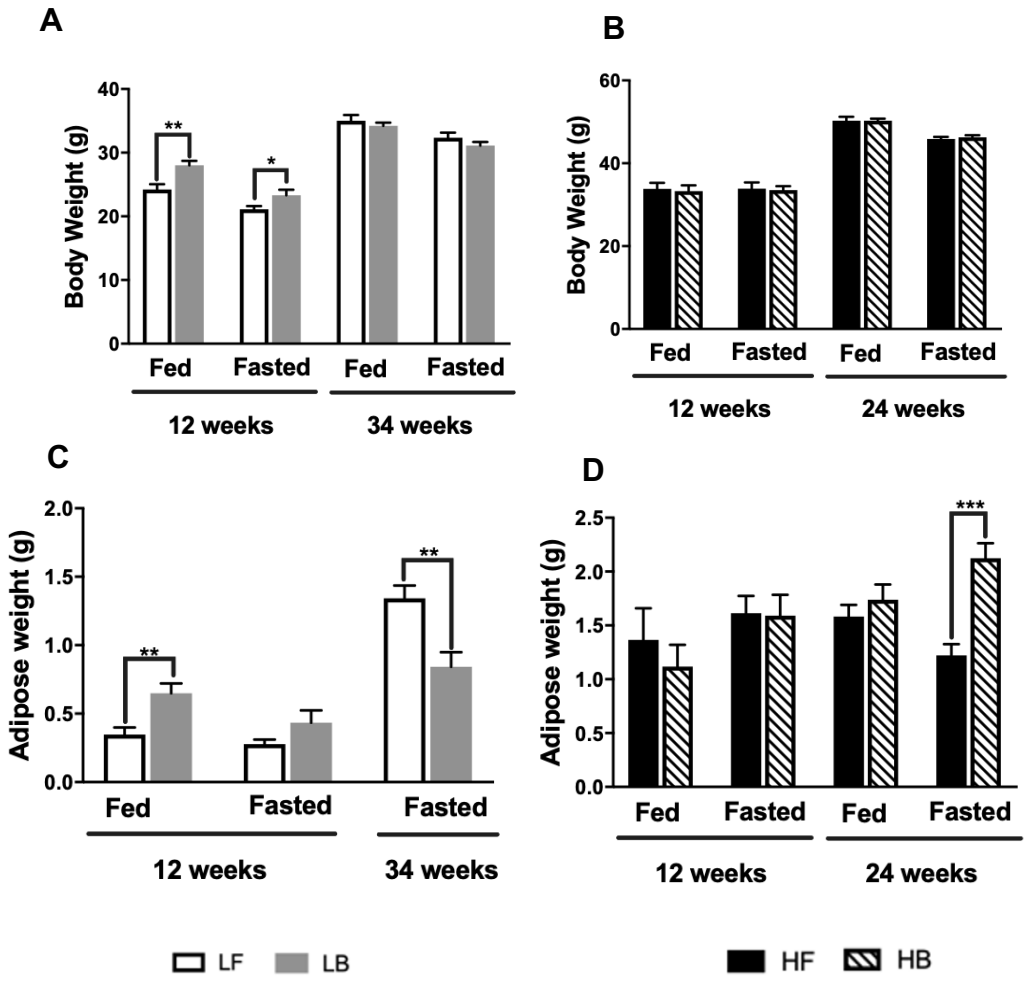

Figure 7: A) Fed and fasted body weights of LF and LB groups after 12 and 34 weeks on their respective diets, **B)** Fed and fasted body weights of HF and HB groups after 12 and 24 weeks on their respective diets, **C)** Fed and fasted perigonadal WAT weights after 12 weeks on the diets and fasted perigonadal WAT weights in LF and LB groups after 34 weeks on the diets **D)** Fed and fasted perigonadal WAT weights of HF and HB groups after 12 and 24 weeks on diet. Data is presented as means ± standard error of means (SEM). n= 6-10 per treatment group. Differences in the means indicated by *p < 0.05, **p<0.01, ***p < 0.001

To determine if BCAA supplementation impacted patterns of lipid storage, six adipose depots were collected from mice on diet for 12 weeks (Figure 8A) and weighed (Figure 8B). These depots represented four adipose depot types: subcutaneous (interscapular and inguinal WAT), visceral (perigonadal and mesenteric WAT), intermuscular (popliteal WAT), and BAT (interscapular BAT). Mice supplemented with BCAAs on a high-fat background had significantly lower perigonadal, mesenteric, and popliteal WAT and lower interscapular BAT (Figure 8B) than the HF control mice. The adipose tissue weights between LF and LB groups were not statistically different from each other.

Over the course of dietary feeding, the animals feed intake and body weights were measured weekly. During 12 weeks on diet, the LB group maintained higher body weights (Figure 9E) compared to LF. After 34 weeks on diet, supplemented animals consumed more feed and kilo-calories on average per day (Figure 10A and B) compared to their LF counterparts. In the high-fat groups, HF caloric intake is higher than HB at 12 weeks (Figure 11B). Extension of the time on the custom diets to 24 weeks exacerbated differences in caloric intake and revealed decreased feed intake in BCAA supplemented animals (Figure 12A and B) compared to their control counterparts.

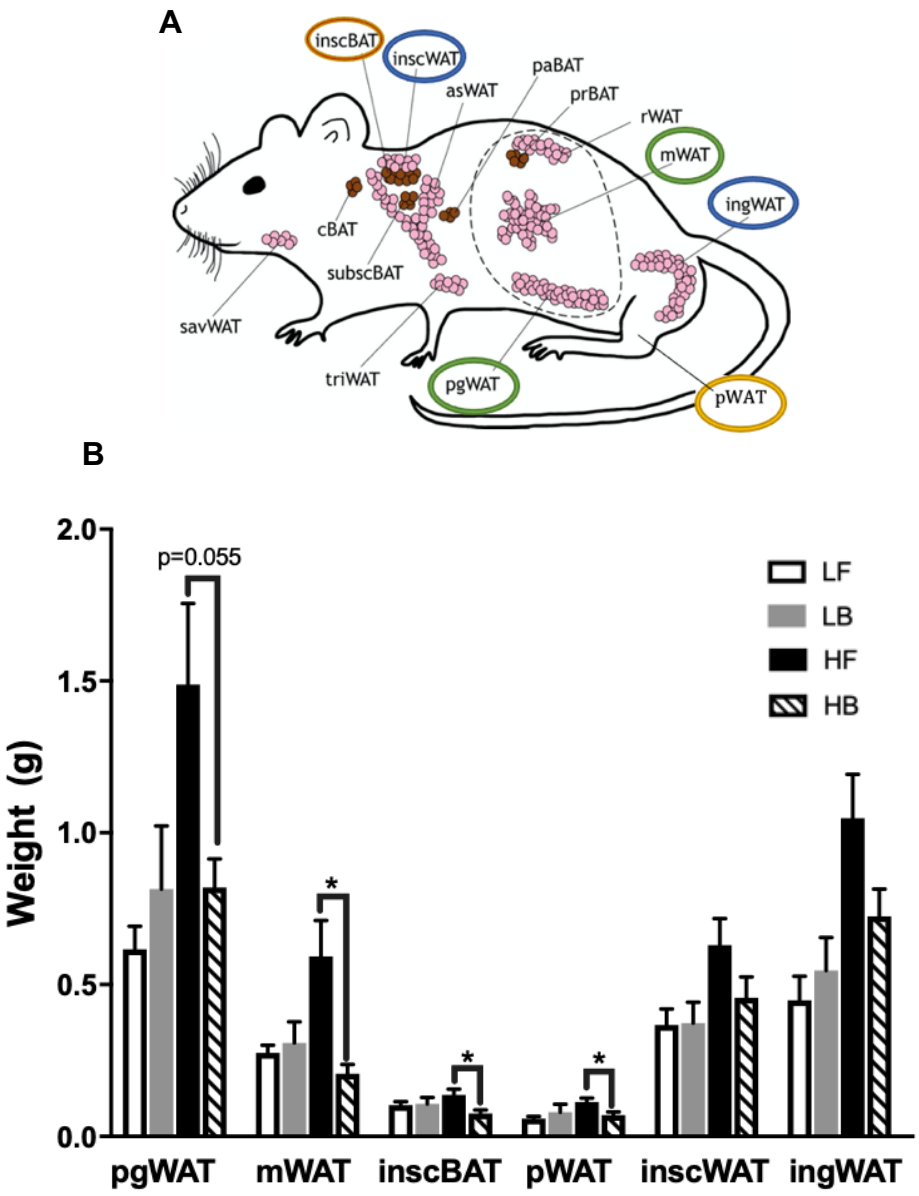

Figure 8: A) Image depicting the 6 murine adipose depots weighed. inscBAT - interscapular BAT, inscWAT - interscapular WAT, mWAT - mesenteric WAT, ingWAT - inguinal WAT, pWAT - popliteal WAT, pgWAT - perigonadal WAT **B)** Weight (g) of adipose depots. Data is presented as means ± SEM. n= 6 per treatment group. Differences in the means indicated by *$p < 0.05$.

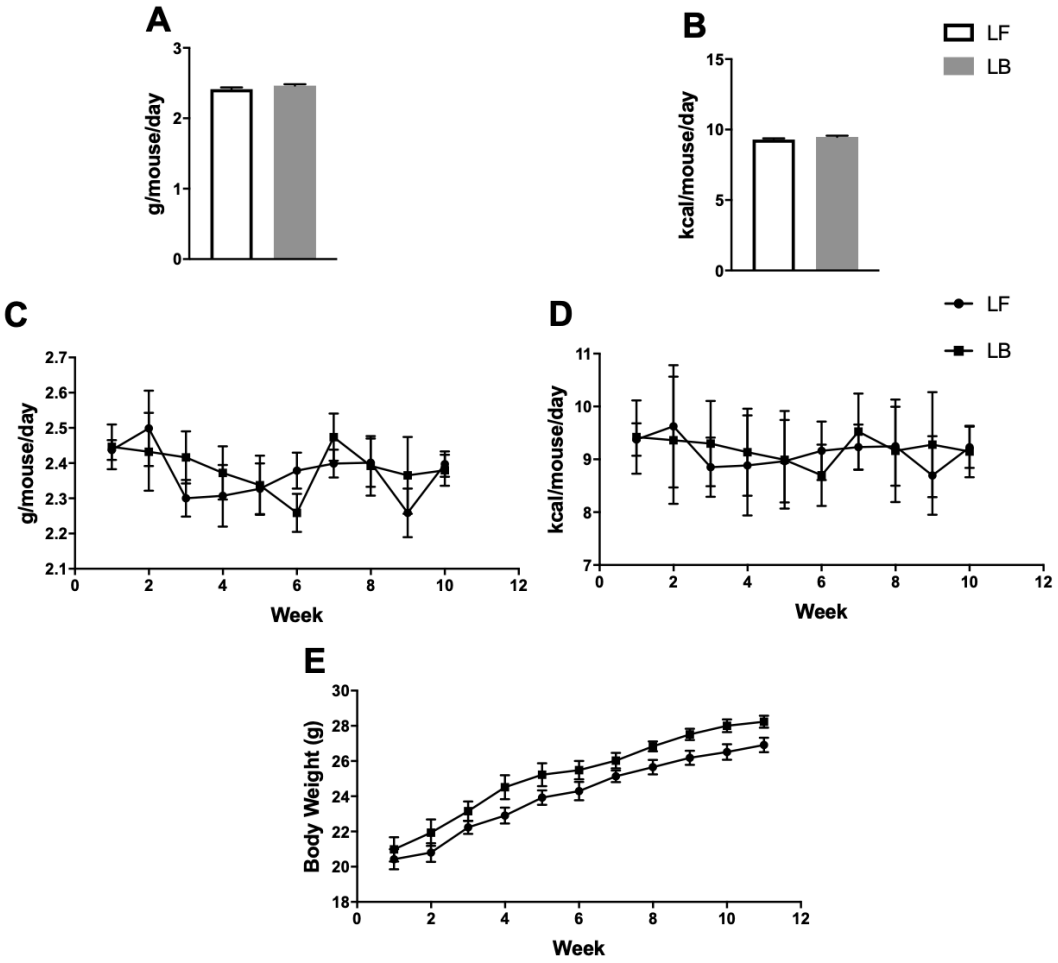

Figure 9: LF and LB feed intake and body weights over 12 weeks of dietary intervention. **A)** Average grams of feed consumed per mouse per day, **B)** Average kcal consumed per mouse per day, **C)** Average grams of feed consumed per mouse per day over 12 weeks on custom diets, **D)** Average kcal consumed per mouse per day over 12 weeks on custom diets, **E)** Body weight over 12 weeks on custom diets. Data is presented as means ± SEM. n=10 per treatment group.

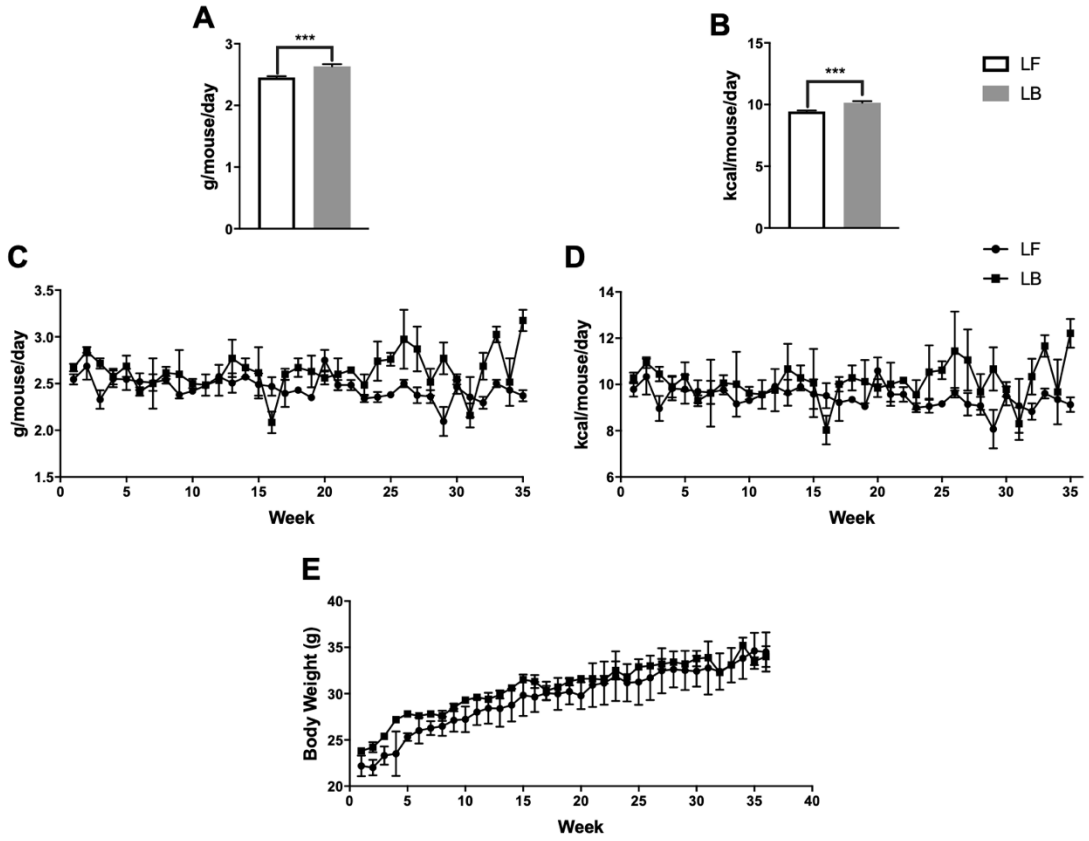

Figure 10: LF and LB feed intake and body weights over 34 weeks of dietary intervention. **A)** Average grams of feed consumed per mouse per day, **B)** Average kcal consumed per mouse per day, **C)** Average grams of feed consumed per mouse per day over 34 weeks on custom diets, **D)** Average kcal consumed per mouse per day over 34 weeks on custom diets, **E)** Body weight over 34 weeks on custom diets. Data is presented as means ± SEM. n=35 per treatment group. Differences in the means indicated by ***$p < 0.001$.

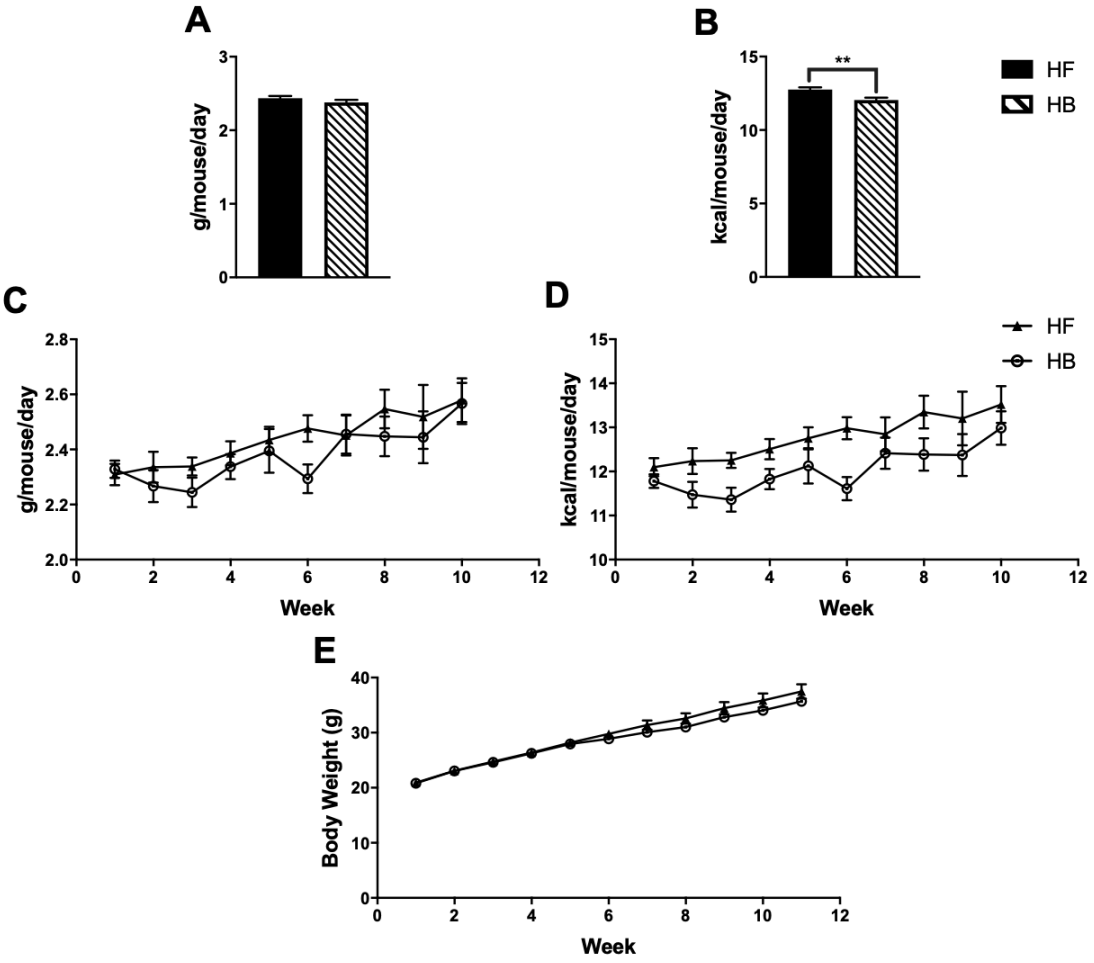

Figure 11: HF and HB feed intake and body weights over 12 weeks of dietary intervention. **A)** Average grams of feed consumed per mouse per day, **B)** Average kcal consumed per mouse per day, **C)** Average grams of feed consumed per mouse per day over 12 weeks on custom diets, **D)** Average kcal consumed per mouse per day over 12 weeks on custom diets, **E)** Body weight over 12 weeks on custom diets. Data is presented as means ± SEM. n=10 per treatment group. Differences in the means indicated by $^{**}p < 0.01$.

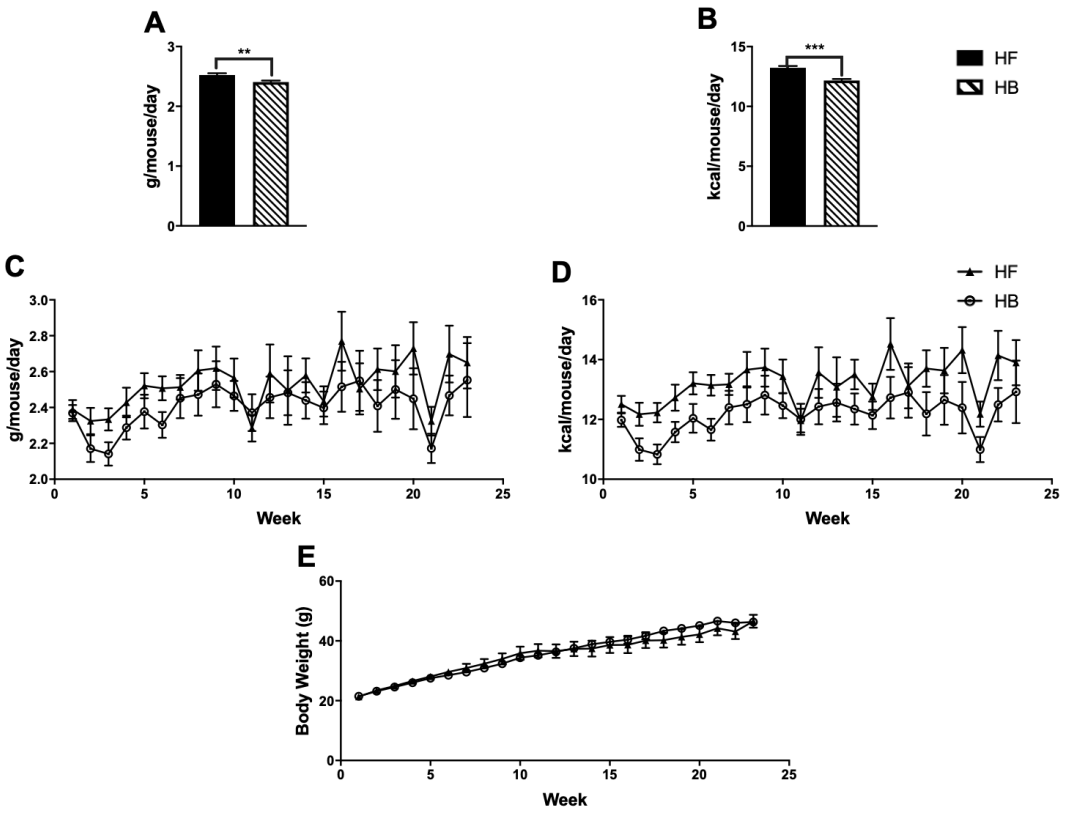

Figure 12: HF and HB feed intake and body weights over 24 weeks of dietary intervention. **A)** Average grams of feed consumed per mouse per day, **B)** Average kcal consumed per mouse per day, **C)** Average grams of feed consumed per mouse per day over 24 weeks on custom diets, **D)** Average kcal consumed per mouse per day over 24 weeks on custom diets, **E)** Body weight over 24 weeks on custom diets. Data is presented as means ± SEM. n=23 per treatment group. Differences in the means indicated by **$p < 0.01$, ***$p<0.001$

To determine whether these animals are insulin resistant, serum insulin c-peptide were measured using a ELISA assays (Crystal Chem). After 12 weeks on diet and following fasting, the HF and HB animals demonstrate a trend of higher circulating insulin and c-peptide compared to the low-fat groups (Table 12). Insulin levels in the HF and HB groups after 24 weeks of supplementation are elevated even further. LB animals that were supplemented for 34 weeks had significantly lower insulin levels after fasting than LF.

Adiponectin, a hormone that has been recognized to positively impact insulin sensitivity, was not significantly different between the four groups after 12 weeks of dietary intervention (Table 12).

Leptin is a starvation hormone that, when its concentration falls below a certain threshold, signals the brain to stimulate more feed intake. Leptin also is closely related to insulin resistance. After 12 weeks on the custom diets, fed HF mice demonstrated significantly higher leptin levels than their supplemented counterparts (Table 12).

Morphological differences in adipose tissue were observed by histological analysis. In the WAT of mice on the custom diets for 12 weeks, LB animals appeared to have larger white adipocytes than the LF (Figure 13A). The opposite trend is seen in HB, where smaller adipocytes are present compared to HF (Figure 13B). In BAT, even stronger differences in lipid accumulation and adipose expansion are noted. Both the LB and HB groups demonstrate reduced lipid droplet size and number compared to their control diet counterparts (Figure 14A and B).

Table 11

Serum Insulin and C-Peptide Analysis

Insulin (ng/mL)	LF	LB	HF	HB
12wks, Fed	0.46 ± 0.12	0.52 ± 0.08	0.48 ± 0.08	0.41 ± 0.06
12wks, Fasted	0.12 ± 0.01	0.14 ± 0.02	0.29 ± 0.07	0.22 ± 0.05
34/24wks, Fed	--	--	10.37 ± 1.92	6.49 ± 1.54
34/24wks, Fasted	0.28 ± 0.04[a]	0.19 ± 0.02[a]	1.07 ± 0.12	2.26 ± 0.56
C-Peptide (ng/mL)				
12wks, Fed	0.49 ± 0.05	0.58 ± 0.09	0.62 ± 0.11	0.52 ± 0.08
12wks, Fasted	0.17 ± 0.05	0.16 ± 0.04	0.31 ± 0.09	0.29 ±0.05

Note. Serum insulin and C-peptide profile of LF and LB mice after 12 and 34 weeks of supplementation and HF and HB mice after 12 and 24 weeks of supplementation. Data is presented as means ± SEM. n= 6 per treatment group. Results with the same superscript letter are statistically significant from each other ($p < 0.05$).

Table 12

Serum Hormone Analysis

Serum Hormone	LF	LB	HF	HB
Adiponectin (µg/mL, fed)	7.33 ± 0.37	6.6 ± 0.46	5.92 ± 0.22	5.59 ± 0.28
Leptin (ng/mL, fed)	6.03 ± 0.81	6.03 ± 2.26	15.07 ± 3.35[b]	5.04 ± 1.83[b]

Note. Serum adiponectin and leptin concentrations for mice on diet for 12 weeks and in the fed condition. Data is presented as means ± SEM. n= 6 per treatment group. Results with the same superscript letter are statistically significant from each other ($p < 0.05$).

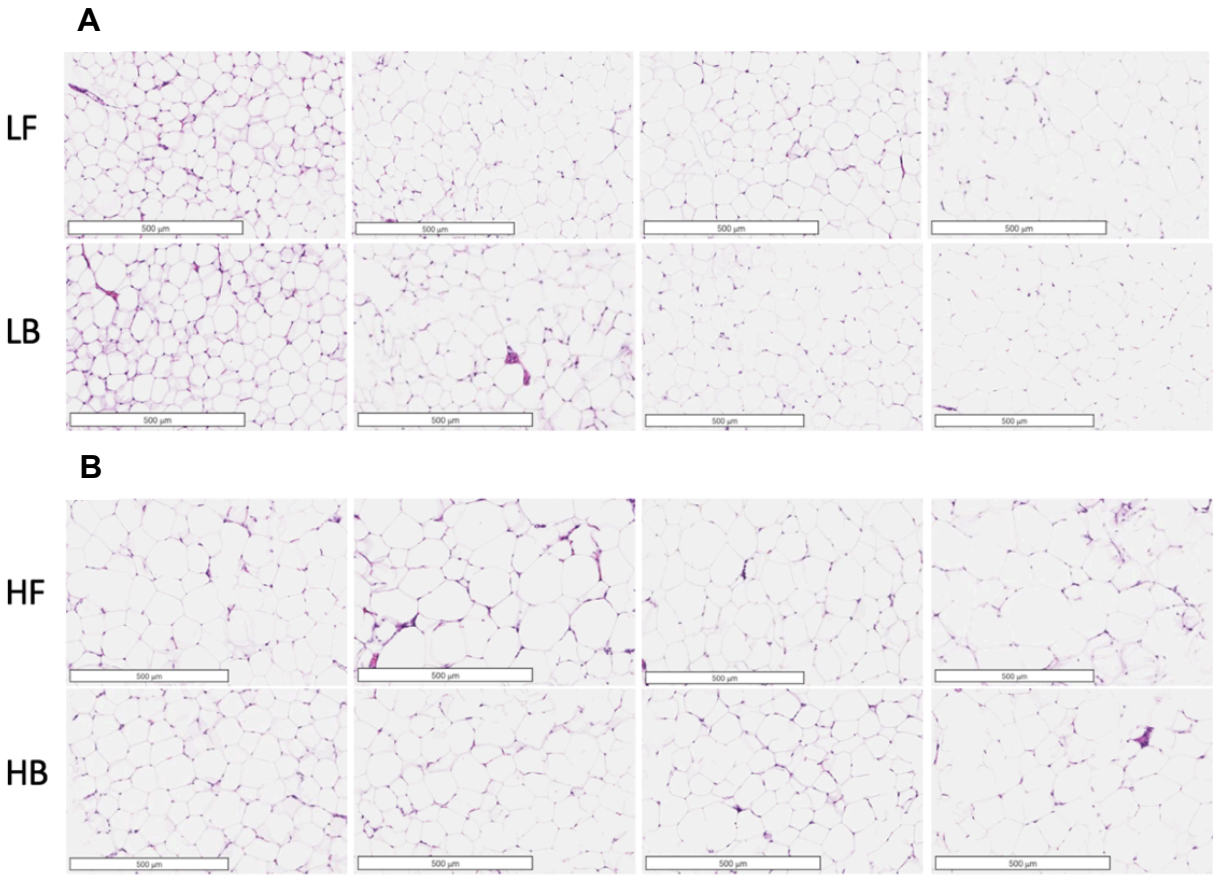

Figure 13: Perigonadal WAT from mice on custom diets for 12 weeks and in the fed condition. Tissue was stained using H&E and imaged at 5x magnification **A)** LF and LB comparison, **B)** HF and HB comparison. n=4 per group

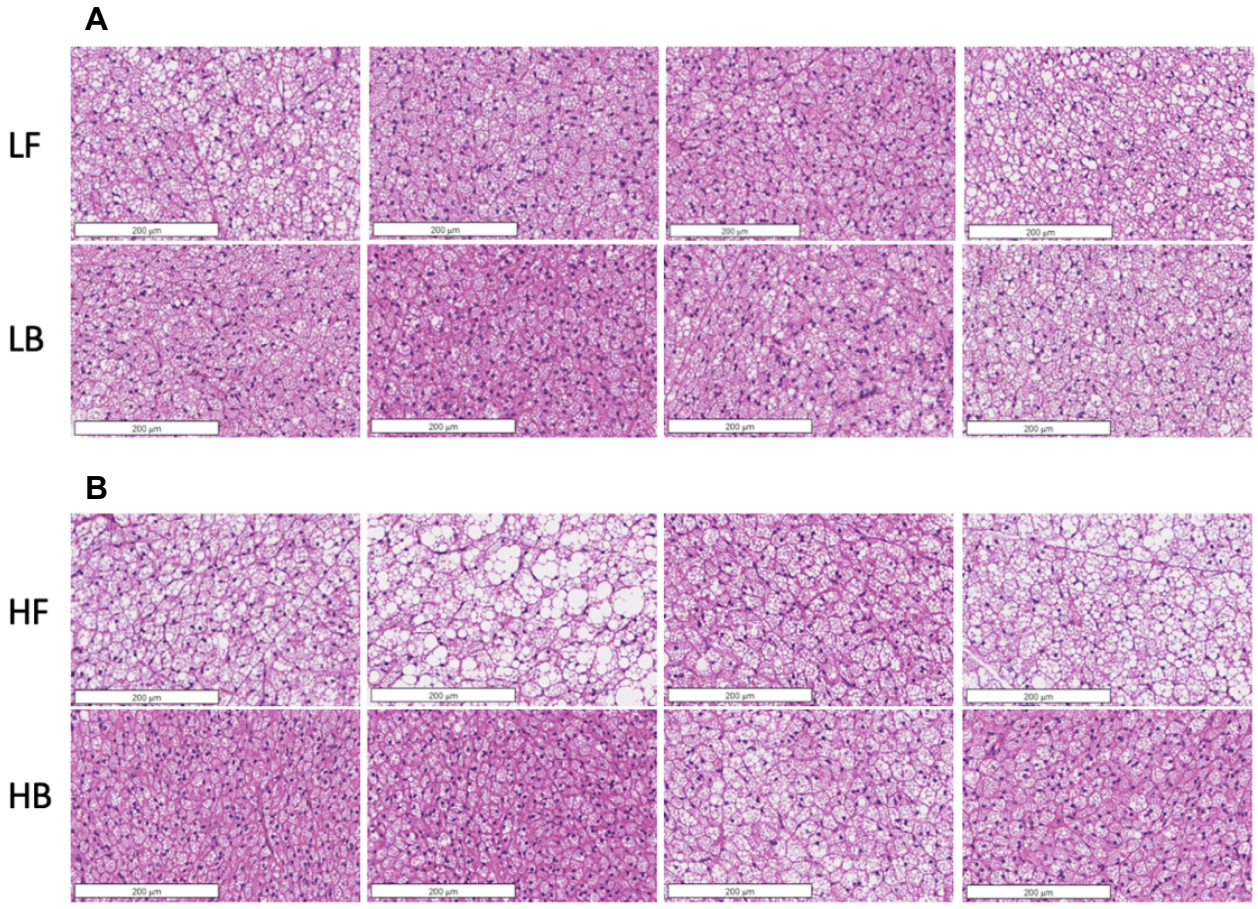

Figure 14: Interscapular BAT from mice on custom diets for 12 weeks and in the fed condition. Tissue was stained using H&E and imaged at 10x magnification **A)** LF and LB comparison, **B)** HF and HB comparison. n=4 per

Objective 2: BCAA Degradation and Mitochondrial Function

To determine whether BCAA degradation rates were impacted by BCAA supplementation, we first looked at amino and keto acid concentrations in the perigonadal WAT of mice on custom diets for 12 weeks and in the fed condition. In the LB group, all of the BCAAs and their respective keto acids were significantly higher than LF (Figure 15A and C). While not all the measurements in the HF and HB animals were significant, the trends were the same as the low-fat group comparisons (Figure 15B and D). These trends of higher BCAAs and keto acids are a promising indicator that there is more BCAA degradation occurring in the supplemented tissues.

To substantiate the GC-MS data and further study the BCAA degradation pathway, three genes were measured for their relative expression using qPCR. Branched-chain aminotransferase (*Bcat2*) performs the first step of BCAA degradation. Branched chain keto acid dehydrogenase kinase (*Bckdk*) inhibits the activity of the second BCAA degradation enzyme, BCKDH. The third gene, peroxisome proliferator activated receptor-gamma (*Pparγ*), upregulates BCAA degradation when activated. For all four groups, there were no significant differences in gene expression (Figure 16A and B).

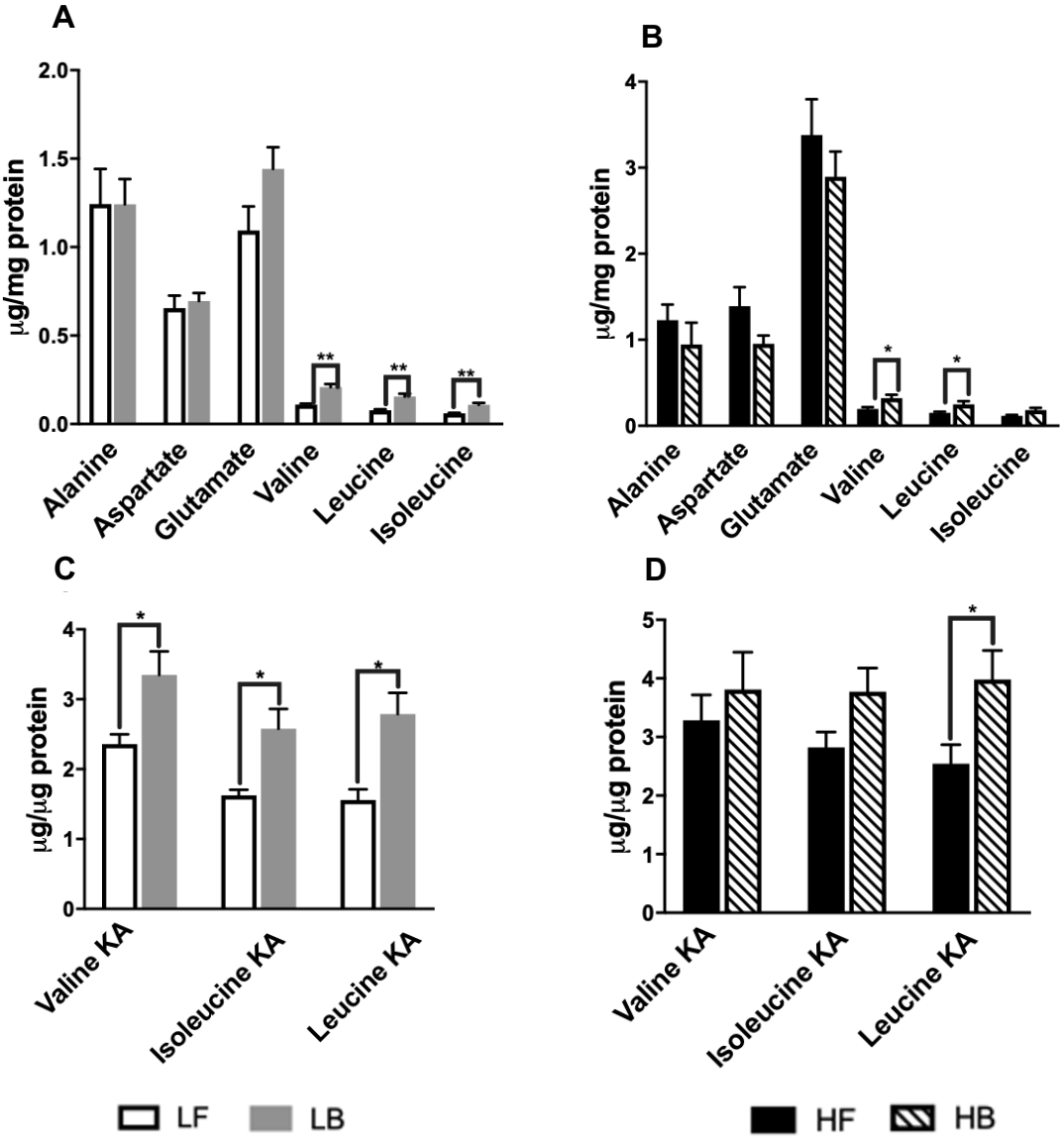

Figure 15: Targeted metabolomics of amino acids and keto acids in perigonadal WAT from mice on custom diets for 12 weeks and in the fed condition **A)** Amount of amino acids in WAT of LF and LB animals **B)** Amount of amino acids in WAT of HF and HB animals **C)** Amount of keto acids in WAT of LF and LB animals **D)** Amount of keto acids in WAT of HF and HB animals. Data is presented as means ± SEM. n=6 per treatment group. Differences in the means indicated by *$p < 0.05$

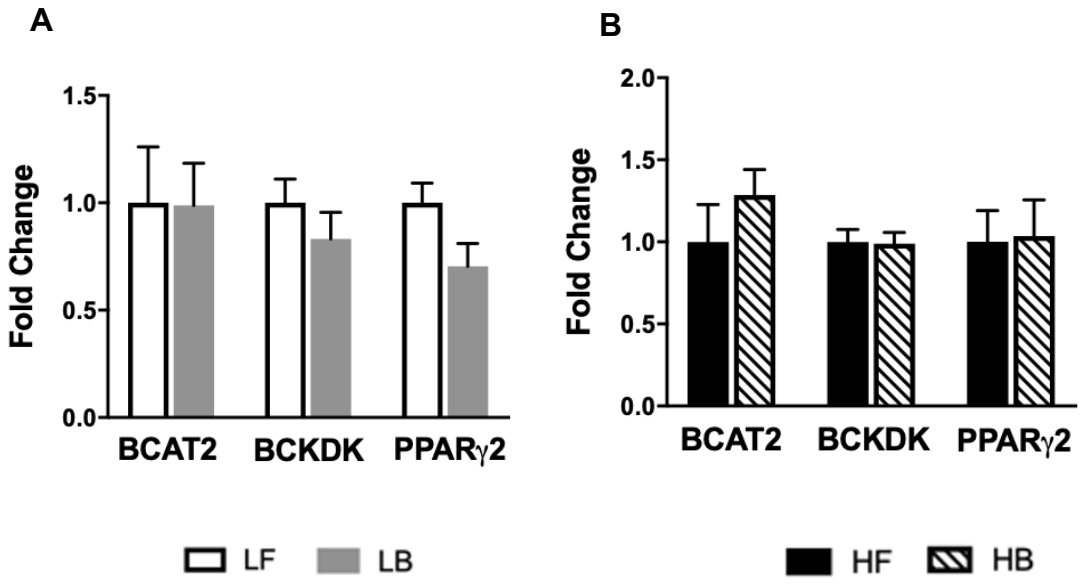

Figure 16: Perigonadal WAT qPCR analysis of BCAA degradation gene expression of fed, 12 week supplemented animals. Data is expressed as fold change compared to the control diet (LF or HF) **A)** LF and LB gene expression **B)** HF and HB gene expression. Data is presented as means ± SEM. n=5-6 per treatment group.

BCAA degradation and mitochondrial function are closely linked characteristics of obesity, T2DM, and NAFLD. We wanted to study if BCAA supplementation would impact adipocyte mitochondrial function. To do this, we measured tri-carboxylic acid (TCA) cycle intermediates using GC-MS. In perigonadal WAT of mice on custom diets for 12 weeks and in the fed condition, all four groups showed no significant differences in TCA cycle intermediates (Figure 17A and B).

Protein expression of the electron transport chain complexes (OXPHOS) and cytochrome-C oxidase (COXIV) were measured by western blot analysis as another measure of mitochondrial function. There were no significant differences between LF and LB or HF and HB (Figures 18 and 19) mice that were on custom diets for 12 weeks.

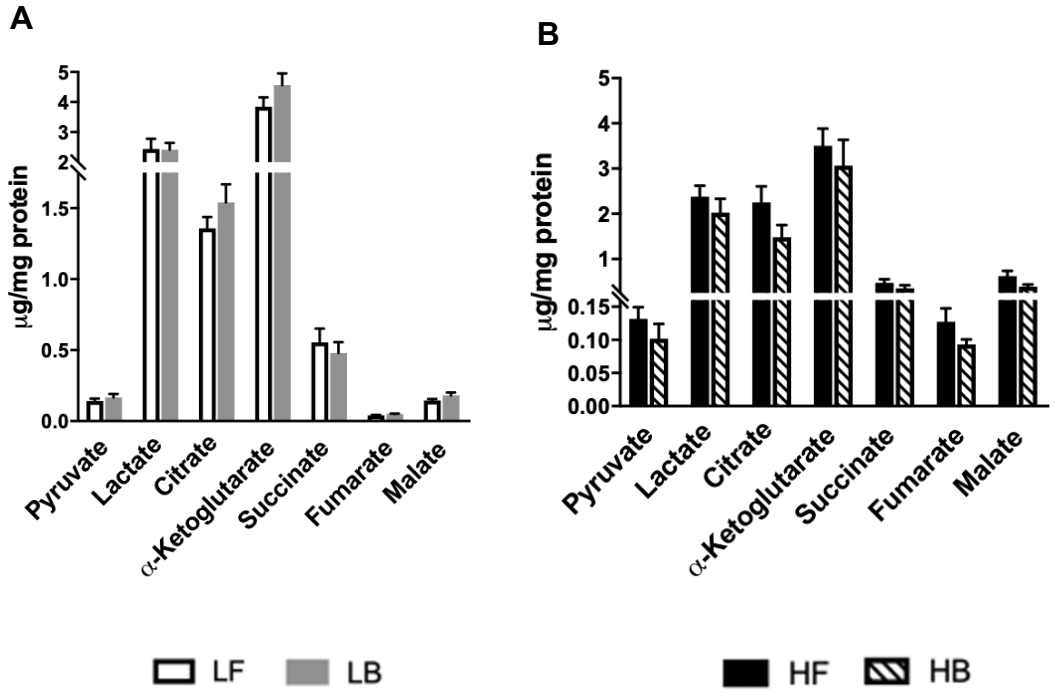

Figure 17: Targeted metabolomics of organic acids in perigonadal WAT of 12 mice on custom diets for 12 weeks and in the fed condition **A)** Amounts of organic acids in LF and LB groups **B)** Amounts of organic acids in HF and HB groups. Data is presented as means ± SEM. n=6 per treatment group.

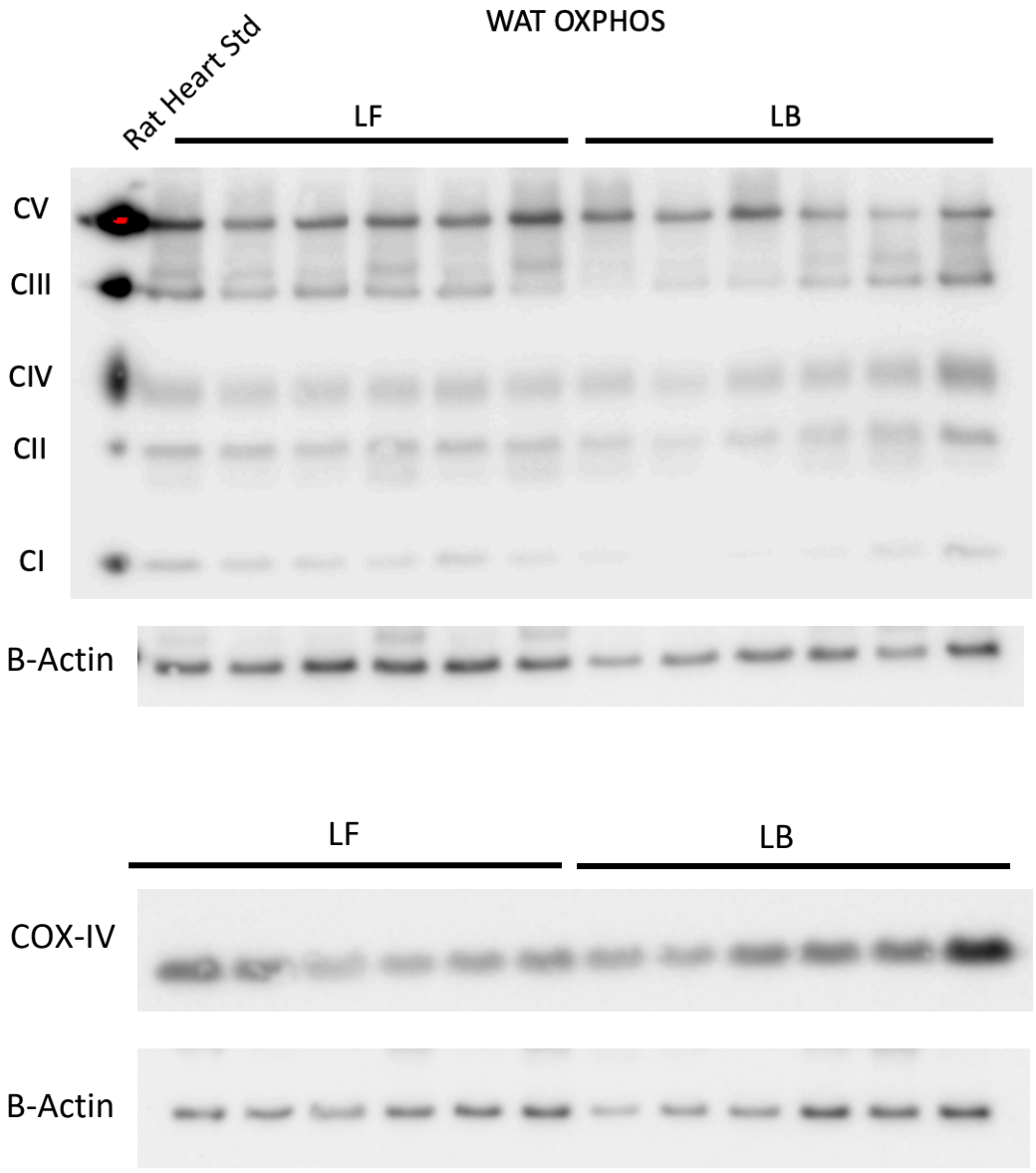

Figure 18: Western blots of mitochondrial proteins associated with the electron transport chain expressed in perigonadal WAT of mice on custom diets for 12 weeks and in the fed condition. n=6 per treatment group.

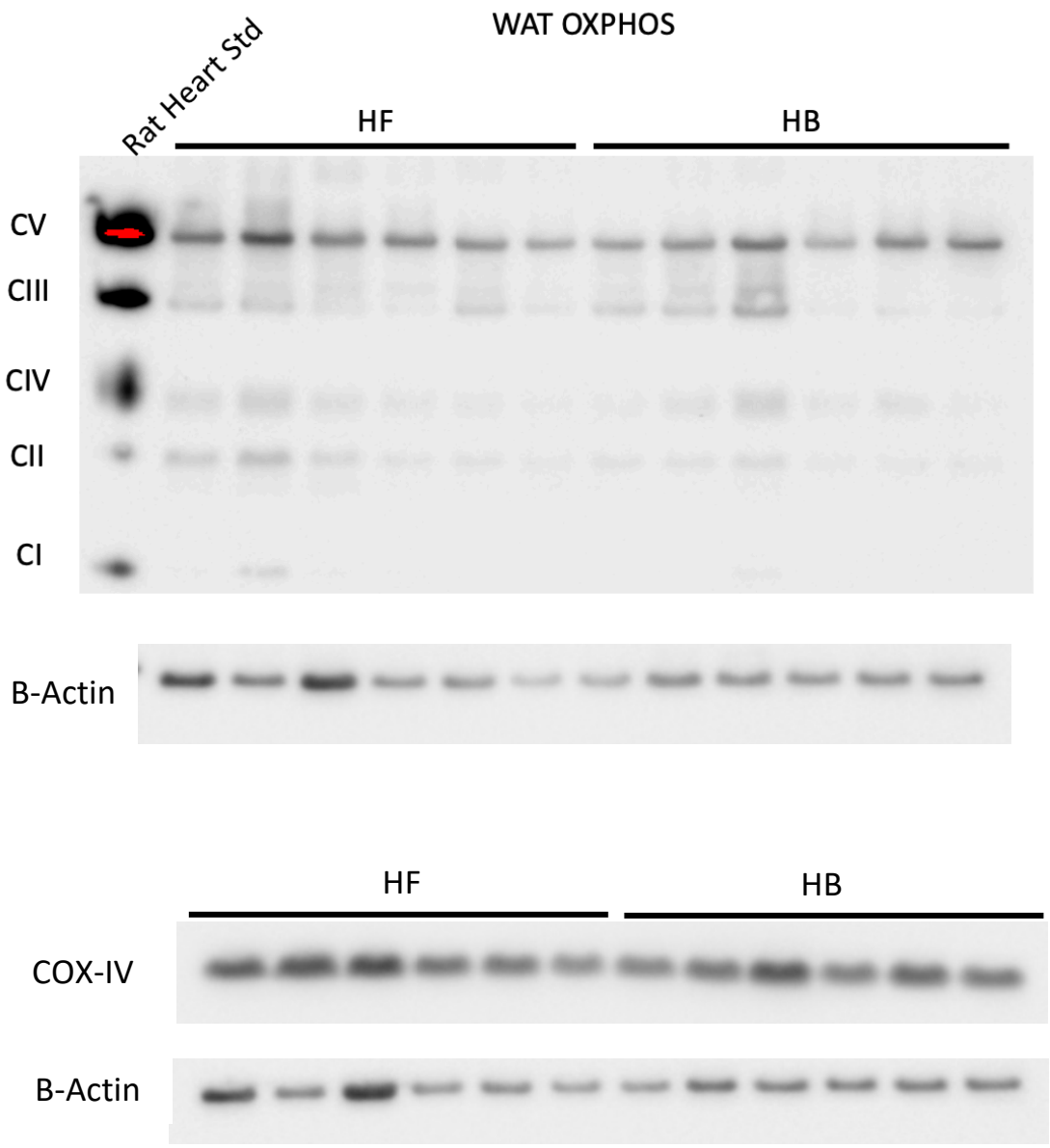

Figure 19: Western blots of mitochondrial proteins associated with the electron transport chain expressed in perigonadal WAT of mice on custom diets for 12 weeks and in the fed condition. n=6 per treatment group.

The same battery of experiments were conducted in interscapular BAT to measure BCAA degradation and mitochondrial function. GC-MS analysis was conducted to measure amino acids in the interscapular BAT of animals on custom diets for 12 weeks. LB animals trended to have higher amino acids than LF (Figure 20A). The HB group had significantly more glutamate, valine, leucine, and isoleucine than HF (Figure 20B). The keto acids appeared higher in the LB group (Figure 20C), as well as in HB mice (Figure 20D) compared to their control counterparts.

For gene expression after 12 weeks on custom diets, we used qPCR to measure the interscapular BAT gene expression of *Bcat2*, *Pgc1α*, and *Ucp1*. *Bcat2* is the first enzyme in the BCAA degradation pathway. *Pgc1α* is a transcription co-activator that induces mitochondrial biogenesis and is activated during cold stress. Lastly, *Ucp1* is the thermogenesis protein that utilizes lipids and BCAAs for heat production. There were no significant differences in gene expression between the low-fat groups (Figure 21A) or high-fat groups (Figure 21B).

TCA cycle intermediates were measured by GC-MS in interscapular BAT of mice on custom diets for 12 weeks. LB animals had significantly higher pyruvate and trended to have higher amounts of intermediates than LF (Figure 22A). HF and HB animals were not statistically different from each other (Figure 22B).

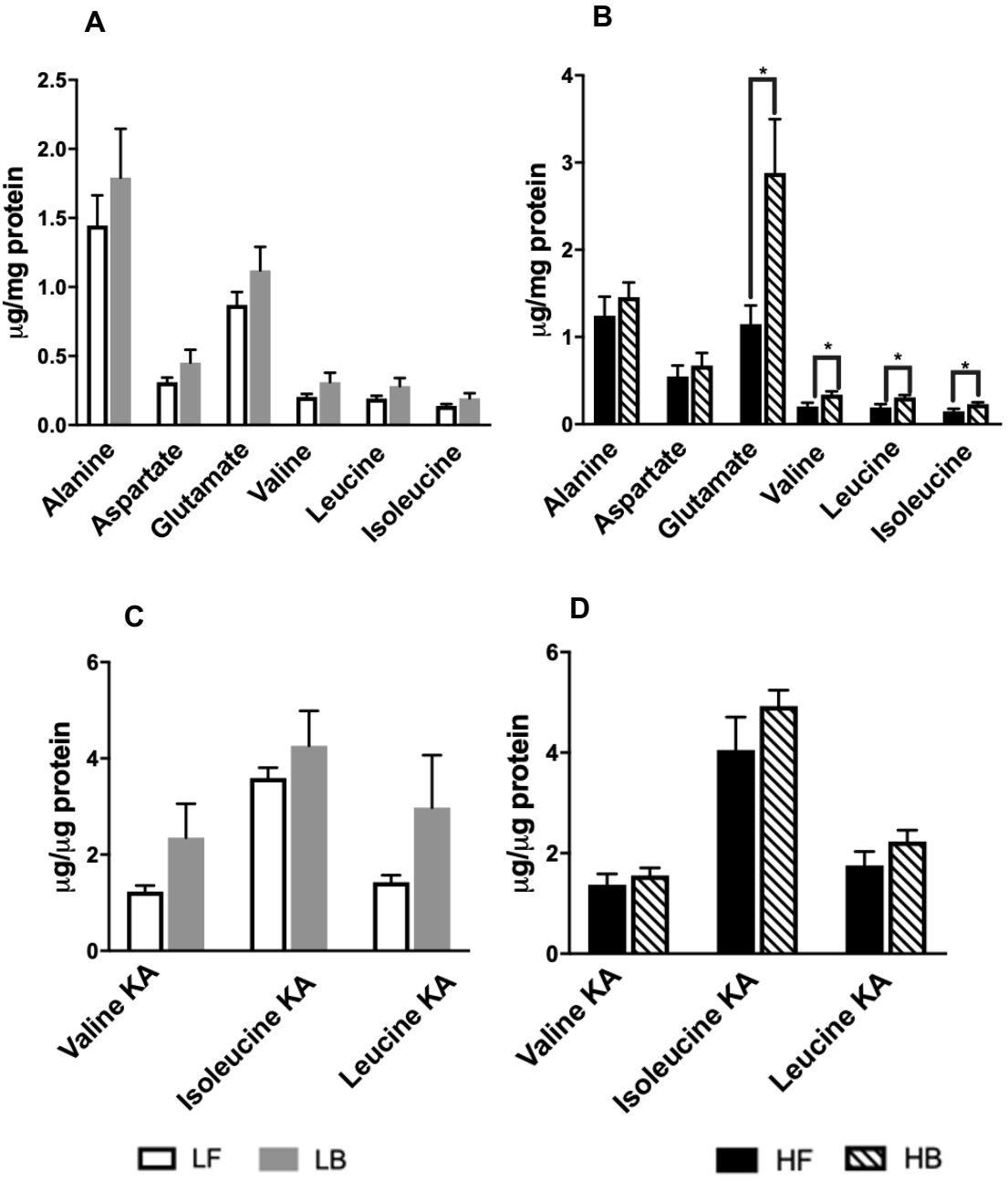

Figure 20: Targeted metabolomics of amino acids and keto acids in interscapular BAT from mice on custom diets for 12 weeks and in the fed condition. **A)** Amount of amino acids in BAT of LF and LB animals, **B)** Amount of amino acids in BAT of HF and HB animals, **C)** Amount of keto acids in BAT of LF and LB animals, **D)** Amount of keto acids in BAT of HF and HB animals. Data is presented as means ± SEM. n=6 per treatment group. Results were considered significant at *$p < 0.05$

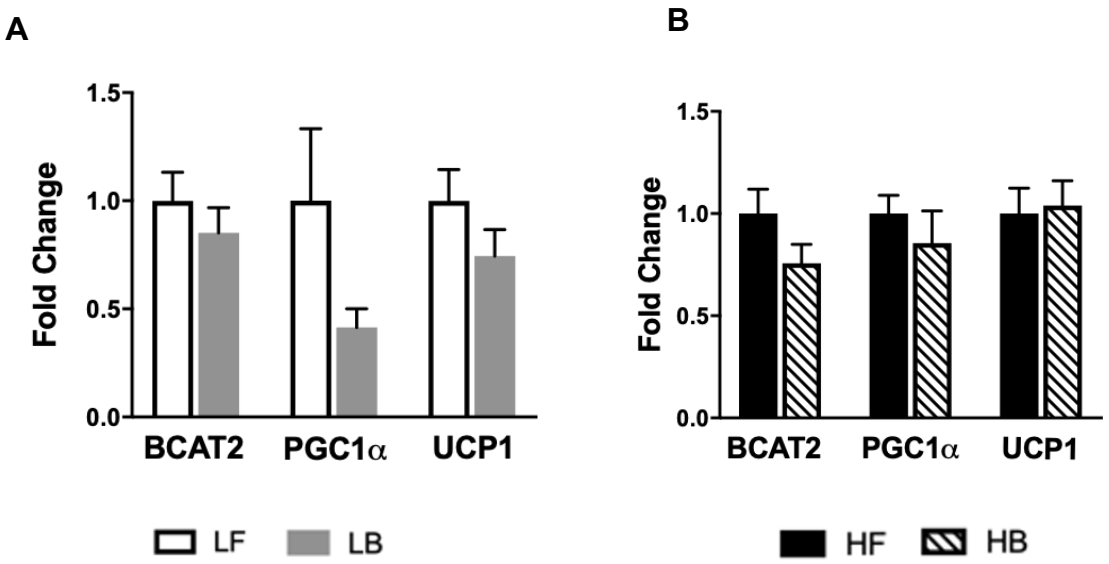

Figure 21: Interscapular BAT qPCR analysis of BCAA degradation and thermogenesis gene expression of mice on custom diets for 12 weeks and in the fed condition. **A)** LF and LB gene expression **B)** HF and HB gene expression. Data is presented as means ± SEM. n=5-6 per treatment group.

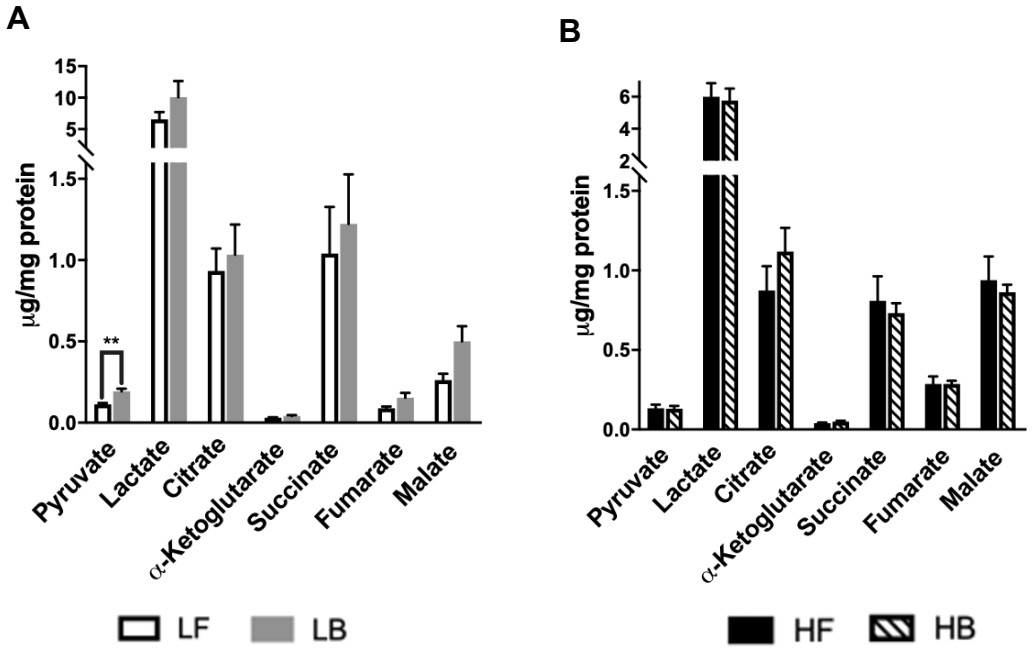

Figure 22: Targeted metabolomics of organic acids in interscapular BAT from mice on custom diets for 12 weeks and in the fed condition. **A)** Amounts of organic acids in LF and LB groups **B)** Amounts of organic acids in HF and HB groups. Data is presented as means ± SEM. n=5-6 per treatment group. Results were considered significant at $^{**}p < 0.01$.

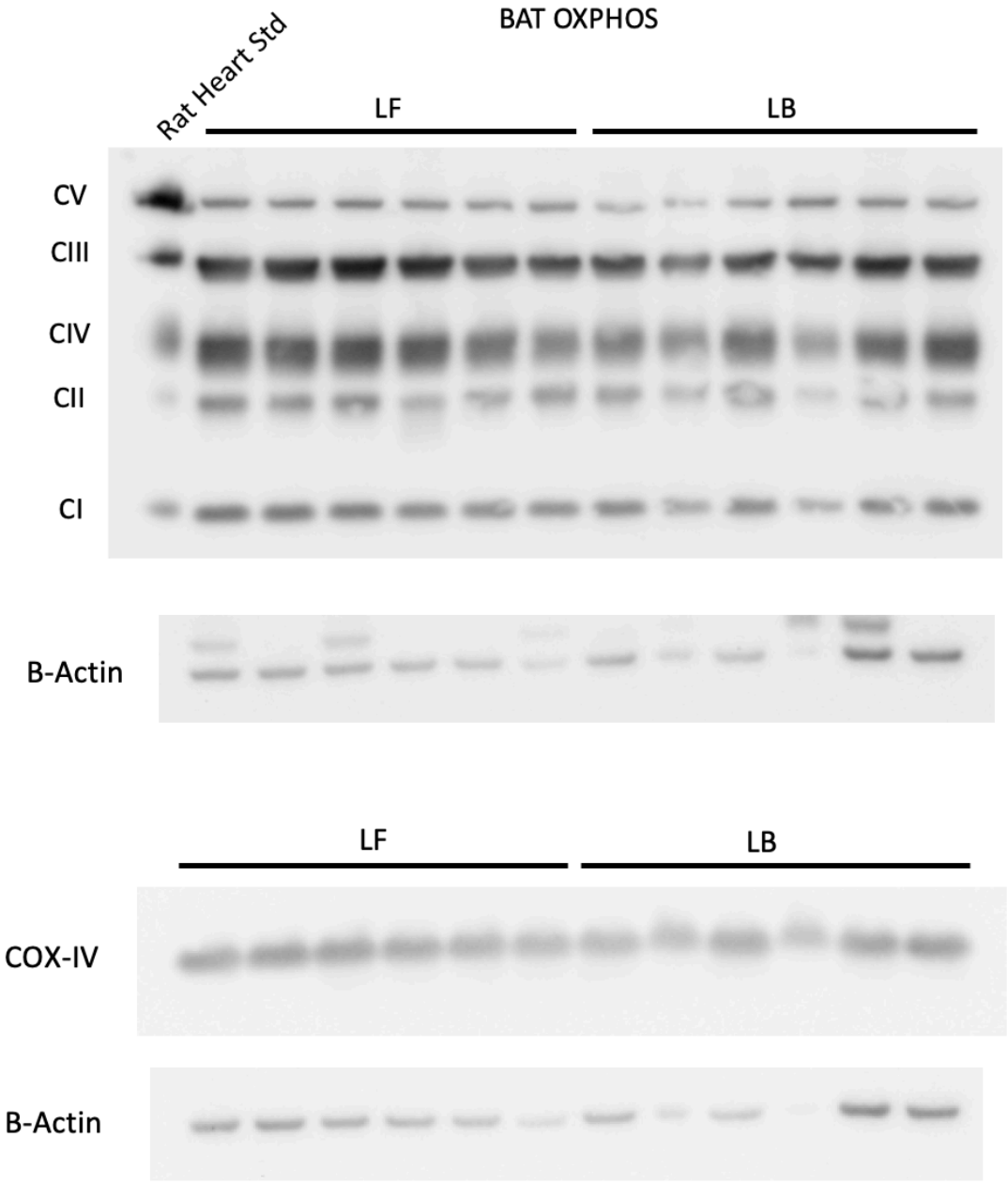

Figure 23: Western blots of mitochondrial proteins associated with the electron transport chain expressed in interscapular BAT of mice on LF and LB diets for 12 weeks and in the fed condition. n=6 per group.

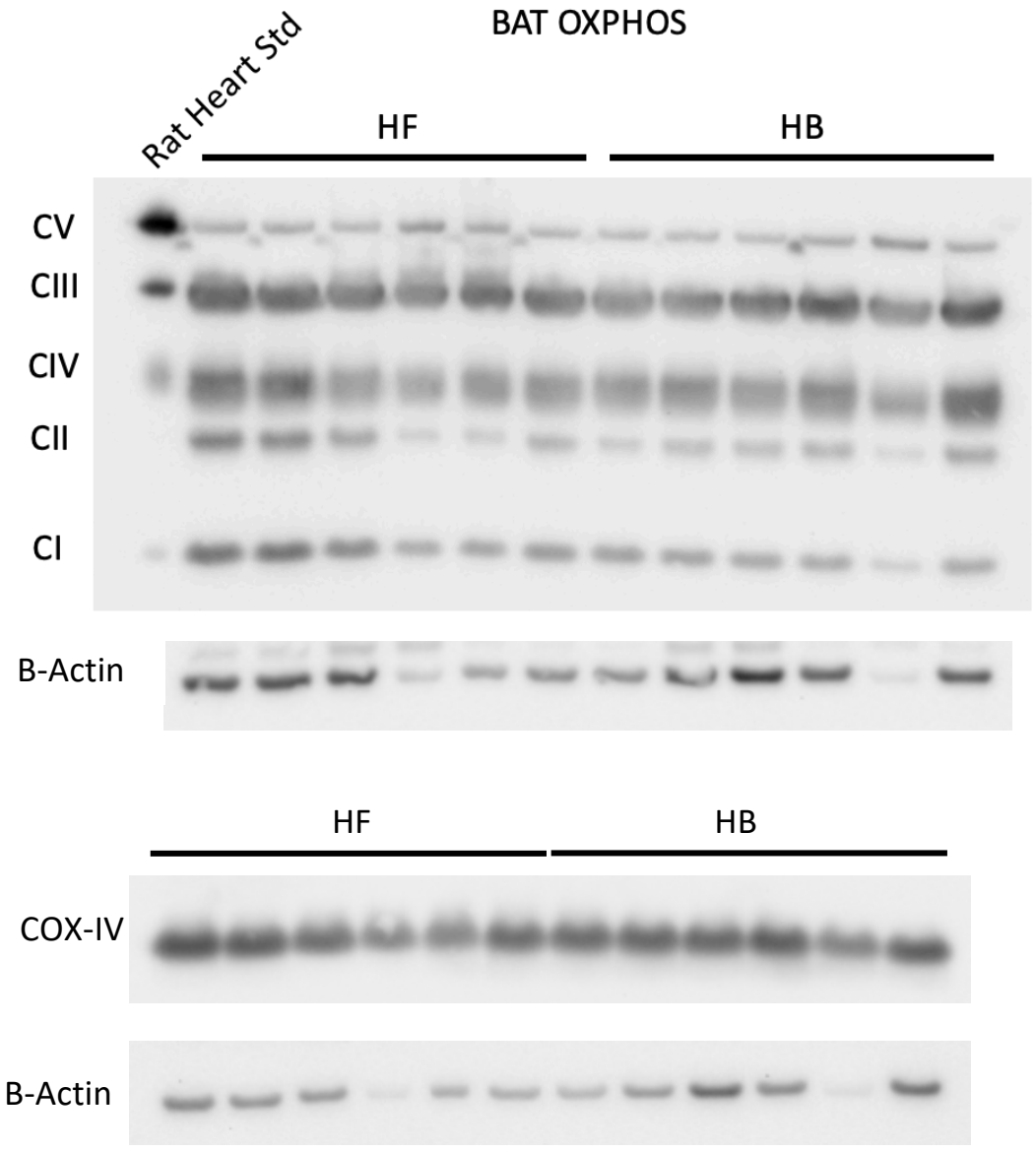

Figure 24: Western blots of mitochondrial proteins associated with the electron transport chain expressed in interscapular BAT of mice on HF and HB diets for 12 weeks and in the fed condition. n=6 per group

Objective 3: Impact of BCAAs on Lipolysis

We measured higher serum non-esterified free fatty acids (NEFA) in the 34 week LB group compared to LF (Figure 25A), while no difference in serum NEFA was measured between the 24 week HF and HB groups (Figure 25B). To determine if the elevated circulating free fatty acids in the LB group were due to increased adipose tissue lipolysis, we performed an *in vitro* lipolysis assay using perigonadal WAT explants. Explants were incubated in a media with or without 5μM isoproterenol at 37°C and 5% CO_2.

Lipolysis releases both fatty acids and glycerol, so both were measured in the lipolysis assay media. The LB group showed trends of increased basal fatty acid release (Figure 25A). Isoproterenol was very effective at inducing lipolysis and increased fatty acid release, however there were no differences between the LF and LB groups in the stimulated condition. The LF group had a significantly higher basal to stimulated fold change compared to LB. There were no significant differences in HF and HB fatty acid release (Figure 25B). To substantiate this data, glycerol in the media was also measured. The basal glycerol release in the LB group is significantly higher than LF, which agrees with the fatty acid trend. In the HB group, glycerol release in the basal treatment was significantly lower.

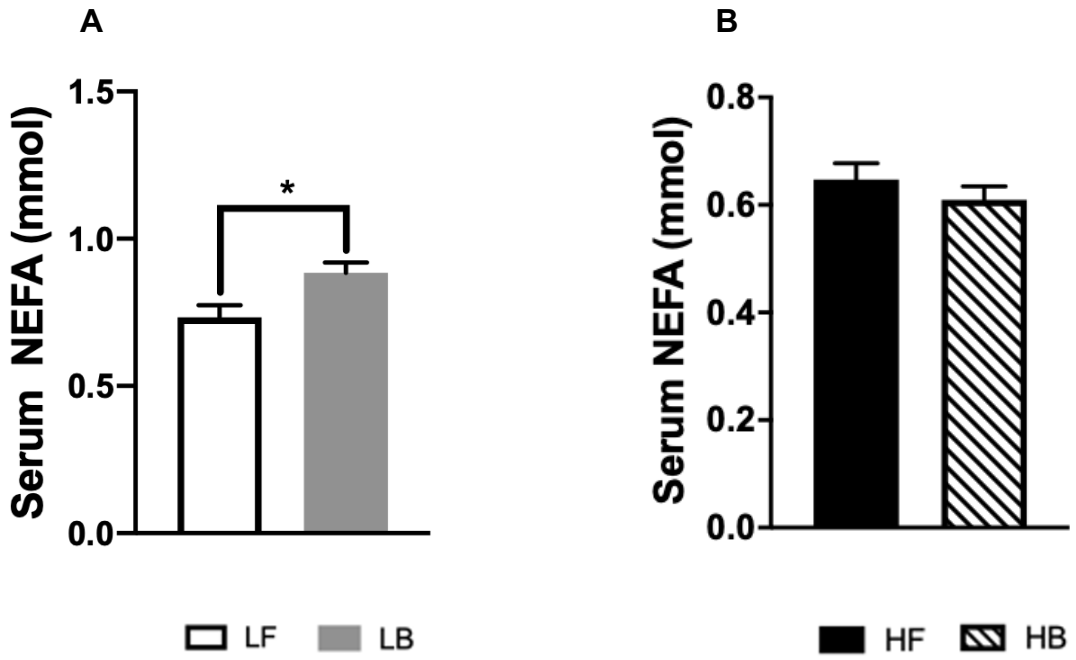

Figure 25: Serum non-esterified fatty acids (NEFA) in **A)** 34 week LF and LB groups and **B)** 24 week HF and HB groups. Data is presented as means ± SEM. n=8-10 per treatment group. Results were considered significant at *$p < 0.05$.

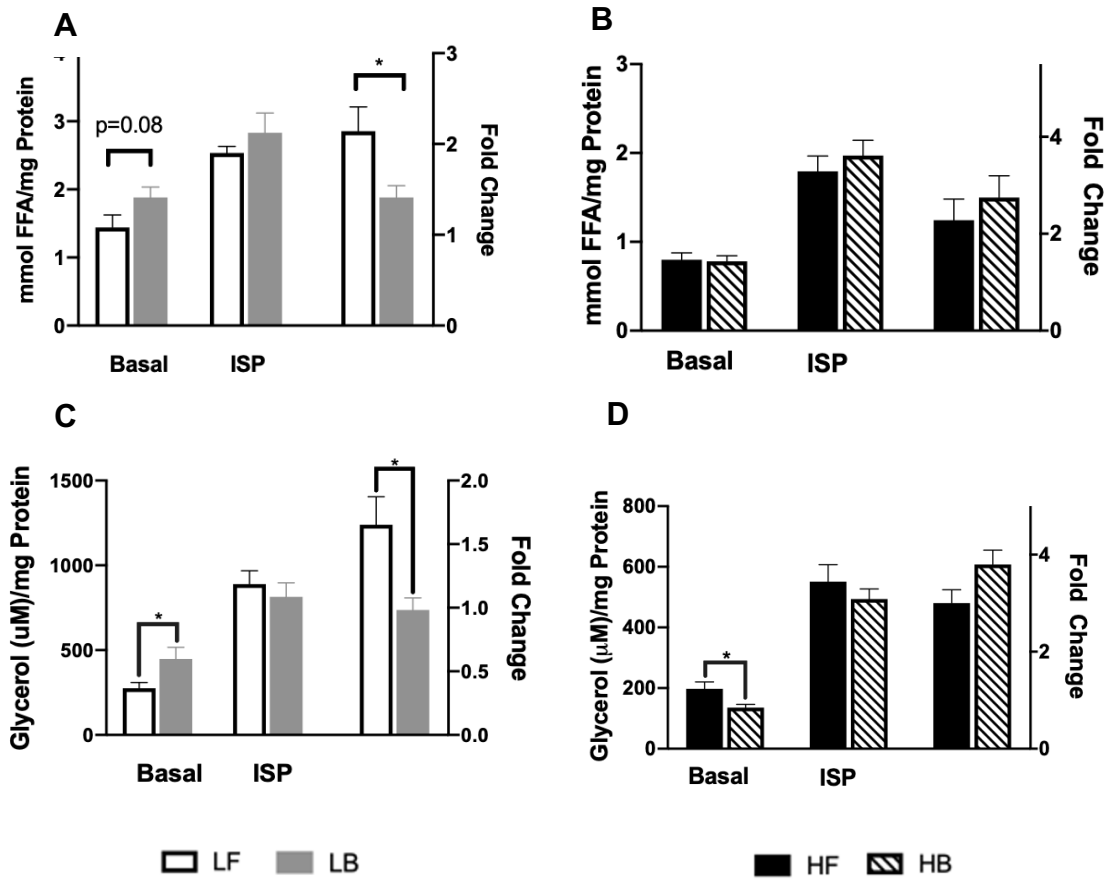

Figure 26: *In vitro* lipolysis assay results from fasted, LF and LB mice on custom diets for 34 weeks and fasted, HF and HB mice on custom diets for 24 weeks. **A)** LF and LB concentrations of free fatty acids released in lipolysis assay media **B)** HF and HB concentrations of free fatty acids released in lipolysis assay media **C)** LF and LB glycerol release into lipolysis assay media **D)** HF and HB glycerol release into lipolysis assay media. Data is presented as means ± SEM. n=8-10 per treatment group. Results were considered significant at *$p < 0.05$.

If our hypothesis is that BCAA supplementation will induce lipolysis, then directly treating the adipose explants with BCAAs should also induce lipolysis. For this set of experiments, perigonadal WAT explants from fasted mice on diets for 12 week were incubated in a media with 500μM and 1mM BCAAs. Consistently across all four groups, higher BCAA concentrations in the media induced increased fatty acid release into the media (Figure 27). To further support this trend, another lipolysis assay was performed on normal, chow fed mice. For this experiment, perigonadal WAT was incubated in basal and 2.5μM ISP media with 50μM, 500μM, 1mM, or 2.5mM BCAAs. This was to test if BCAAs could sustain a higher lipolytic rate following stimulation. While the results are inconclusive, the trend of higher basal to stimulated fold changes among the three highest BCAA concentrations is promising (Figure 28).

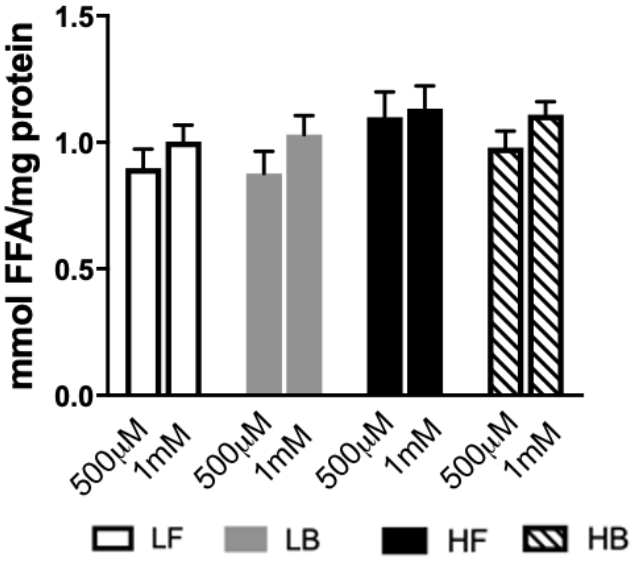

Figure 27: *In vitro* lipolysis assay free fatty acid release from fasted, 12 week supplemented mice treated with 500µM and 1mM BCAAs. Data is presented as means ± SEM. n=8-10 per treatment group.

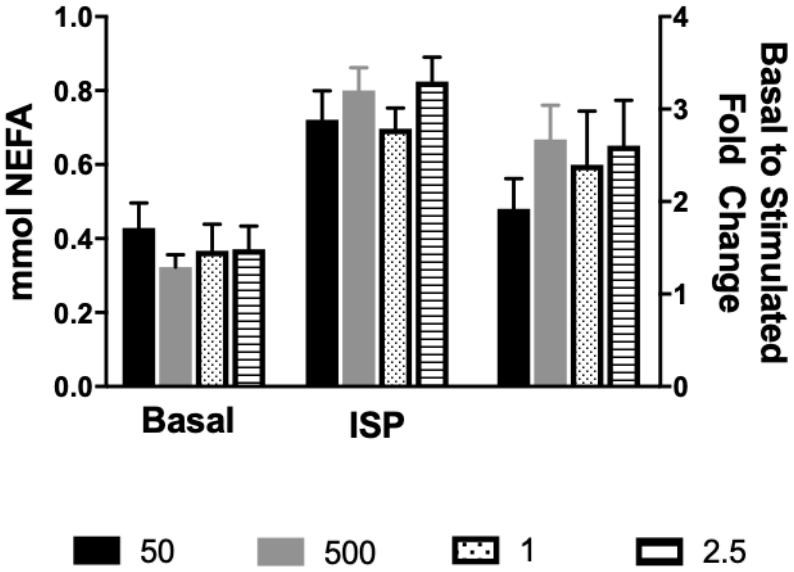

Figure 28: *In vitro* lipolysis assay fatty acid release of pgWAT explants from normal, chow-fed mice treated with 50µM, 500µM, 1mM, and 2.5 mM BCAAs. Data is presented as means ± SEM. n=6 per treatment group.

Chapter 5: Discussion

Impacts of BCAA Supplementation on Adipose Tissue Morphology and Development

Supplementation of BCAAs resulted in changes to the body weights and adipose tissue phenotype. After 12 weeks on diet, the LB mice had heavier body and perigonadal WAT weights compared to their LF controls (Figure 7A and C). Consistent with our observations, Ribeiro et al. demonstrates a correlation between high circulating BCAAs and increased adipose and body weight in mice (2019). Given that these are young, growing mice, supplementing BCAAs could also have preferentially impacted their growth rate and protein synthesis. The HF and HB animals, on the other hand, maintained similar body weights and perigonadal WAT weights after 12 weeks on the custom diets. However after 24 weeks on these diets, HB animals had significantly higher perigonadal WAT weights following an overnight fast (Figure 7D). This was contrary to our expectations that during the feeding to fasting transition, the adipose weight will decrease as a consequence to high rates of lipolysis. The higher perigonadal adipose tissue weights after fasting in HB mice highlights the differential regulation of the adipose tissue phenotype following BCAA supplementation and warrants further investigation.

The dynamic interaction between BCAAs and adipose depot weights was futher illustrated by the observations that the HB animals maintained on custom diets for 12 weeks, under fed conditions, mantained significantly lower visceral, BAT, and intermuscular adipose weights than the HF mice. No significant difference was

measured in subcutaneous depot weights between the HF and HB mice (Figure 8B). The size of visceral adipose depots is correlated to metabolic health, as individuals with large visceral adipose depots are thought to be more metabolically unhealthy. On the other hand, those with large subcutaneous depots tend to be more insulin sensitive and have a decreased risk of developing metabolic diseases including T2DM (Mittal, 2019). After BCAA supplementation, not only is the overall adipose tissue weight reduced in HB animals, but there appears to be preferential lipid storage away from the visceral adipose tissue depots. Comparing the relative visceral to subcutaneous adipose weights, this could be a mechanism by which BCAAs are protecting the BCAA supplemented mice from the progressive severity of metabolic disease.

Significant differences in feed intake was also observed following CAA supplementation. After 34 weeks of dietary BCAA supplementation, LB animals consumed significantly more food on both grams and kilo-calories per day basis (Figure 10A and B). This was in spite of the fact that the LB mice adipose weights were significantly lower than LF (Figure 7A). These results could indicate that the LB animals have higher metabolic rates and a higher efficiency to divert these calories towards oxidation as opposed to storage as lipids.

In the HF and HB groups, differences in average kcal of feed consumed after 12 weeks on the diets was significantly different, but no changes in the amount of feed consumed were observed (Figure 11B). This is likely because of the initial differences in calorie density between the HF and HB diets (Table 1). Since the HB diet inherently contains less kcal per gram, consuming the same grams of feed would equate to the HB animals obtaining less calories. After 24 weeks on diet, however, we see not only less

calories being consumed by HB animals, but also significantly lower feed intake (Figure 12A and B). This is no longer a matter of calorie density of the diets, but a significant reduction in the amount of food the HB mice are consuming. This trend in food intake is interesting considering the results that the perigonadal adipose tissue weights of the HB mice were significantly higher after fasting. These trends comparing the HF and HB mice are also opposite of the trend observed in the 34 week LF and LB mice. In the HB group, these mice consume significantly less feed, but maintain larger perigonadal WAT weight. It is widely understood that altering protein content in a diet impacts appetite. Generally, low dietary protein induces hyperphagia (Laeger et al., 2014) while high amounts of protein satiate more readily (Bensaïd et al., 2003). While both LB and HB animals are supplemented with higher levels of BCAAs, our results suggest that insulin resistance in the HB animals can differentially impact food intake and adipose tissue accretion.

In the context of normal physiology, insulin levels should readily decrease in response to fasting and rise following feeding. During insulin resistance, fasted levels of insulin will remain high due to the system being unable to efficiently clear circulating glucose and would be even higher during feeding due to insulin resistance. There were no significant differences in the fed insulin and c-peptide levels between the four groups of mice after 12 weeks on custom diets (Table 11). In the fasted condition, however, it is noted that the HF and HB groups insulin concentrations begin to remain elevated compared to the low-fat groups, indicating that these animals may be in the early stages of developing insulin resistance. The measured serum c-peptide concentrations agree with this observation. Extending the dietary treatments to 24

weeks resulted in a significant increase in serum insulin levels in both HF and HB groups compared to the LF and LB counterparts. In the HF and HB groups, serum insulin concentrations are very high in the fed condition compared to the 12 week values. This shows these animals require higher amounts of insulin to maintain glucose homeostasis. Once fasted, the insulin levels do decrease, but not to the extent of the 12 week animals. It is clear that these HF and HB animals are insulin resistant after 24 weeks of high fat diet feeding and this may be the reason for the opposing trends in feed intake and adipose weight between the LB and HB animals. This indicates that BCAA supplementation impacts physiology differently depending on the presence and severity of insulin resistance.

Leptin is an appetite hormone produced by adipose tissue. When adipose stores are sufficient, leptin levels rise, signaling the hypothalamus to limit feed intake. During starvation, when lipid stores become depleted, leptin levels fall and induce feeding. Also related to insulin resistance, leptin resistance is present during obesity due to the chronic excess nutrient intake (Kelesidis et al., 2010). Although no differences in adiponectin were measured, serum leptin showed some interesting trends (Table 12). In the 12 week HF group circulating leptin levels were significantly higher than HB (Table 12). This indicates the HF animals are developing leptin resistance while the BCAA supplemented animals are maintaining normal leptin levels, similar to the low-fat fed groups. BCAAs could be impacting leptin regulation by some unknown mechanism, and preventing early stages of leptin resistance induced by high-fat feeding.

This leptin data does not agree with the measured feed intake, however. If HB animals have lower leptin levels, that should trigger increased feed intake. At 12 weeks of dietary intervention, we see no differences in feed intake between HF and HB (Figure11A). It appears that these differences in leptin are not the cause for the changes in feed intake. There is likely independent mechanisms by which BCAAs are impacting leptin release and feed intake.

Comparing the perigonadal WAT histology from the fed, 12 week groups, there are slight differences in morphology and adipocyte size between the BCAA supplemented groups and their control counterparts. Adipocyte size appears slightly larger in the LB group compared to LF, however this agrees with the adipose weight (Figure 7C). Similarly, smaller adipocytes are present in the HB group compared to its HF counterpart, and perigonadal adipose weight was lower in the HB group during the fed condition (Figure 7D)

In the BAT histology, there are significant differences in the accumulation of lipids (Figures 8 and 14). Comparing LF and LB, LB animals have less lipid accumulation and smaller, fewer lipid droplets even though they maintained higher BAT weight. Further, HB animals have BAT with lipid droplet sizes that are comparable to the LF and LB groups, compared to higher lipid accumulation in BAT from HF fed mice. The reduction in lipid accumulation, especially in the HB group, is an interesting result, especially considering the recent push to pursue BAT specific therapies for the treatment of T2DM and obesity. If BCAA supplemented tissue has a greater propensity to oxidize lipids, leading to reduced lipid accumulation, that could have implications for the treatment of metabolic diseases.

From this data, it is clear that BCAAs are having an impact on adipose tissue development and morphology. Supplementation of dietary BCAAs impacts adipose tissue weights, preferential lipid storage, feed intake, circulating serum leptin concentrations, and adipose tissue morphology. Because of the differences in perigonadal WAT weight and feed intake in the 34 week LB and 24 week HB mice, it is clear that BCAAs impart different effects on normal and insulin resistant systems. However in the 12 week HF and HB animals, where insulin resistance was in its early stages, BCAAs appear to be protecting the HB mice from metabolic disease progression by reducing visceral depot weights and circulating leptin levels.

BCAA Degradation and Mitochondrial Function

Impairment of BCAA degradation network is a hall mark of diseases like obesity, T2DM, and NAFLD, and is believed to contribute to the increased circulating BCAA levels during these diseases (Zhang et al., 2016). Perigonadal WAT from fed, 12 week BCAA supplemented mice showed increases in the amount of BCAAs and their respective keto acids (Figure 15). This significant increase in BCAAs is proof that the dietary BCAAs are being taken up by the tissues and available to be utilized by the adipocytes. The levels of keto acids indicate BCAA degradation is readily occurring, and at a higher rate than in the control tissues. BCAA degradation impairment has been linked to furthering the progression of metabolic diseases (Siddik & Shin, 2019). Dietary supplementation of BCAAs may protect high-fat diet impairment of BCAA degradation by upregulating the pathway, achieving prolonged BCAA catabolic efficiency compared to high-fat diet counterparts.

To corroborate target metabolomics, the expression of three genes were measured: *Bcat2*, *Bckdk*, and *Pparγ*. *Bcat2* is directly involved in the BCAA degradation pathway, *Bckdk* inhibits BCAA degradation, and *Pparγ* has been shown to regulate BCAA degradation (Blanchard et al., 2018). Although no significant differences in gene expression were measured (Figure 16), many studies have linked BCAAs to changes in gene expression (Heng et al., 2020; Liu et al., 2017). There has also been literature evidencing the down-regulation of BCAA degradation genes due to high-fat feeding (Haydar et al., 2018; Sjögren et al., 2020) Due to the chronic nature of the dietary supplementation, BCAAs may not impact gene expression after a prolonged period of time. A more acute dietary supplementation may be required to see these impacts or directly measuring protein expression and activity.

To study the impacts of BCAA supplementation on mitochondrial function, we used targeted metabolomics to measure TCA cycle intermediates. After 12 weeks on the custom diets, there were no significant differences in TCA intermediates between either LF and LB or HF and HB animals (Figure 17). Western blots measuring the electron transport chain proteins also showed no differences between the groups either (Figures 18 and 19). This data suggests that WAT mitochondrial function was not affected by BCAA supplementation. However, this data was using tissues from animals in fed condition so differences may be better seen using fasted animals or measuring the feeding to fasting transition.

For BAT, GC-MS measurements of amino and keto acids showed trends of increased amino and keto acids in the LB animals (Figure 20A and C). The HB group had significantly more glutamate (a BCAA degradation product), BCAAs, and keto

acids (Figure 20B and C). Again, these trends are promising indications that there is increased degradation occurring in the supplemented tissues.

Yoneshiro et al. has evidenced BCAAs being utilized as substrates by BAT during non-shivering thermogenesis (2019). For BAT qPCR, BCAA degradation and thermogenesis genes were measured. We again measured Bcat2, which is directly involved in BCAA degradation. We also measured Pgc1α and *Ucp1* as thermogenic genes. Similar to WAT, there were no differences in gene expression between any of the groups (Figure 21). Once again, due to the chronic supplementation changes in gene expression may not be sustained for the full dietary supplementation.

Shifting our focus to mitochondrial function in BAT, LB animals had significantly more pyruvate and trended to have higher intermediates than their LF controls (Figure 22A). This could indicate higher TCA cycle flux, and may be related to the decreased lipid accumulation seen in the BAT histology (Figure 14). Western blots of mitochondrial electron transport chain proteins show no differences between the groups. Similar to WAT, this data suggests no impacts of BCAA supplementation on mitochondrial function, however the comparison of feeding to fasting may present some differences.

Impacts of BCAA supplementation on Adipose Tissue Lipolysis

Extended supplementation of BCAAs for 34 weeks increased fasting serum NEFA levels in LB animals compared to LF (Figure 25A). BCAAs have recently been shown to impact lipolysis (Heng et al., 2020), and are known to impact molecular mediators of lipolysis including AMPK (Coughlan et al., 2013). To see if BCAA

supplementation increases circulating fatty acids through induction of the lipolysis pathway, an *in vitro* lipolysis assay was performed.

LB animals showed increased basal lipolysis rates through higher fatty acid and glycerol release (Figure 26A and C). This agrees with the serum NEFA measurements and indicates that BCAAs can induce lipolysis and are capable of impacting circulating FFA levels in the fasted condition. In the HF and HB mice, where insulin resistance is present, there are no differences in fatty acid release and reduced free glycerol into the incubation media (Figure 26B and D).

Next we tested if directly treating the adipose explants with BCAAs can induce lipolysis. Across all four groups of 12 week supplemented, fasted mice, the 1mM BCAA concentration consistently increased fatty acid release compared to the 500 μM (Figure 27), even though not in a statistically significant manner. This trend suggests that BCAAs can induce lipolysis in a concentration dependent manner. When we attempted this experiment again, with higher BCAA concentrations and isoproterenol stimulation, the results were not as clear. However, a promising trend in the basal to stimulated fold change may suggest that the three highest BCAA concentrations positively impact WATs ability to upregulate lipolysis when stimulated with isoproterenol (Figure 28).

Across all experiments the trend remained fairly consistent that BCAA supplementation or treatment positively impacts lipolysis in normal animals. However when we attempted to demonstrate an increase in lipolysis following a BCAA concentration dependent manner the data was inconclusive.

Summary

The conclusions of this study support our hypothesis that chronic, dietary supplementation of BCAAs does impact adipocyte function in WAT and BAT and that this effect was blunted by severe insulin resistance. Our result indicate that BCAAs positively impact adipocyte function in a normal animal, as well as protecting the system from the early stages of insulin resistance. However, once the disease has progressed in severity, it appears that BCAAs no longer impart these beneficial effects.

Future Directions

This study leaves many questions unanswered, providing several avenues for future studies.

1) There is close relation of PPARγ, BCAA degradation, and adipocyte differentiation (Estrada-Alcalde et al., 2017; Green et al., 2016; Siersbaek et al., 2010). Would dietary supplementation of BCAAs impact adipocyte differentiation?
2) The clear morphological differences in BAT require more study to understand the impacts BCAAs are having. Reduced lipid accumulation could be due to down regulation of lipid storage or upregulation of lipid oxidation, further studies could determine which pathway is responsible for this morphological difference.
3) The differences in circulating leptin concentrations are another area of study. Leptin is released by adipose tissue, so BCAAs are regulating the ability of

adipose to release leptin. Additionally, what other factors could BCAAs be impacting to effect feed intake so significantly, as seen in this study?

4) Finally, it is consistent that BCAAs are impacting lipolysis. The lipolytic pathway is well studied and understood, so measuring the protein and gene expression of the enzymes involved could elucidate a mechanism for this action.

Bibliography

Achari, A. E., & Jain, S. K. (2017). Adiponectin, a Therapeutic Target for Obesity, Diabetes, and Endothelial Dysfunction. *International Journal of Molecular Sciences*, *18*(6). https://doi.org/10.3390/ijms18061321

Bagchi, D. P., & MacDougald, O. A. (2019). Identification and Dissection of Diverse Mouse Adipose Depots. *Journal of Visualized Experiments*, *149*, 59499. https://doi.org/10.3791/59499

Bensaïd, A., Tomé, D., L'Heureux-Bourdon, D., Even, P., Gietzen, D., Morens, C., Gaudichon, C., Larue-Achagiotis, C., & Fromentin, G. (2003). A high-protein diet enhances satiety without conditioned taste aversion in the rat. *Physiology & Behavior*, *78*(2), 311–320. https://doi.org/10.1016/s0031-9384(02)00977-0

Bjørndal, B., Burri, L., Staalesen, V., Skorve, J., & Berge, R. K. (2011). Different Adipose Depots: Their Role in the Development of Metabolic Syndrome and Mitochondrial Response to Hypolipidemic Agents. *Journal of Obesity*, *2011*, e490650. https://doi.org/10.1155/2011/490650

Blanchard, P.-G., Moreira, R. J., Castro, É., Caron, A., Côté, M., Andrade, M. L., Oliveira, T. E., Ortiz-Silva, M., Peixoto, A. S., Dias, F. A., Gélinas, Y., Guerra-Sá, R., Deshaies, Y., & Festuccia, W. T. (2018). PPARγ is a major regulator of branched-chain amino acid blood levels and catabolism in white and brown adipose tissues. *Metabolism*, *89*, 27–38. https://doi.org/10.1016/j.metabol.2018.09.007

Choe, S. S., Huh, J. Y., Hwang, I. J., Kim, J. I., & Kim, J. B. (2016). Adipose Tissue Remodeling: Its Role in Energy Metabolism and Metabolic Disorders. *Frontiers in Endocrinology*, *7*. https://doi.org/10.3389/fendo.2016.00030

Chuang, D., Chuang, J., & Wynn, R. (2006). Lessons from Genetic Disorders of Branched-Chain Amino Acid Metabolism. *The Journal of Nutrition*, *136*, 243S-9S. https://doi.org/10.1093/jn/136.1.243S

Coughlan, K. A., Valentine, R. J., Ruderman, N. B., & Saha, A. K. (2013). Nutrient Excess in AMPK Downregulation and Insulin Resistance. *Journal of Endocrinology, Diabetes & Obesity*, *1*(1), 1008.

Eggleton, J. S., & Jialal, I. (2021). Thiazolidinediones. In *StatPearls*. StatPearls Publishing. http://www.ncbi.nlm.nih.gov/books/NBK551656/

Estrada-Alcalde, I., Tenorio-Guzman, M. R., Tovar, A. R., Salinas-Rubio, D., Torre-Villalvazo, I., Torres, N., & Noriega, L. G. (2017). Metabolic Fate of Branched-Chain Amino Acids During Adipogenesis, in Adipocytes From Obese Mice and C2C12 Myotubes. *Journal of Cellular Biochemistry*, *118*(4), 808–818. https://doi.org/10.1002/jcb.25755

Estrada-Alcalde, Isabela, Tenorio-Guzman, Miriam, Tovar, Armando, Salinas-Rubio, Daniela, Torre-Villalvazo, Ivan, Torres, Nimbe, & Noriega, Lilia. (2016). Metabolic Fate of Branched-Chain Amino Acids During Adipogenesis, in Adipocytes From Obese Mice and C2C12 Myotubes. *Journal of Cellular Biochemistry*, *118*, 808–818. https://doi.org/10.1002/jcb.25755

Gannon, N. P., Schnuck, J. K., & Vaughan, R. A. (2018). BCAA Metabolism and Insulin Sensitivity—Dysregulated by Metabolic Status? *Molecular Nutrition & Food Research*, *62*(6), e1700756. https://doi.org/10.1002/mnfr.201700756

Green, C. R., Wallace, M., Divakaruni, A. S., Philips, S. A., Murphy, A. N., Ciaraldi, T. P., & Metallo, C. M. (2016). Branched chain amino acid catabolism fuels adipocyte differentiation and lipogenesis. *Nat Chem Biol.*, *12*(1), 15–21. https://doi.org/10.1038/nchembio.1961.

Haczeyni, F., Bell-Anderson, K. S., & Farrell, G. C. (2018). Causes and mechanisms of adipocyte enlargement and adipose expansion: Hypertrophy and hyperplasia in adipose. *Obesity Reviews*, *19*(3), 406–420. https://doi.org/10.1111/obr.12646

Haydar, S., Lautier, C., & Grigorescu, F. (2018). BRANCHED CHAIN AMINO ACIDS AT THE EDGE BETWEEN MENDELIAN AND COMPLEX DISORDERS. *Acta Endocrinologica (Bucharest)*, *14*(2), 238–247. https://doi.org/10.4183/aeb.2018.238

Heng, J., Wu, Z., Tian, M., Chen, J., Song, H., Chen, F., Guan, W., & Zhang, S. (2020). Excessive BCAA regulates fat metabolism partially through the modification of m6A RNA methylation in weanling piglets. *Nutrition & Metabolism*, *17*(1), 10. https://doi.org/10.1186/s12986-019-0424-x

Herman, M. A., She, P., Peroni, O. D., Lynch, C. J., & Kahn, B. B. (2010). Adipose Tissue Branched Chain Amino Acid (BCAA) Metabolism Modulates Circulating BCAA Levels. *The Journal of Biological Chemistry*, *285*(15), 11348–11356. https://doi.org/10.1074/jbc.M109.075184

Holeček, M. (2018). Branched-chain amino acids in health and disease: Metabolism, alterations in blood plasma, and as supplements. *Nutrition & Metabolism*, *15*(1), 33. https://doi.org/10.1186/s12986-018-0271-1

Keipert, S., & Jastroch, M. (2014). Brite/beige fat and UCP1—Is it thermogenesis? *Biochimica et Biophysica Acta (BBA) - Bioenergetics*, *1837*(7), 1075–1082. https://doi.org/10.1016/j.bbabio.2014.02.008

Kelesidis, T., Kelesidis, I., Chou, S., & Mantzoros, C. S. (2010). Narrative Review: The Role of Leptin in Human Physiology: Emerging Clinical Applications. *Annals of Internal Medicine*, *152*(2), 93–100. https://doi.org/10.1059/0003-4819-152-2-201001190-00008

Kersten, S. (2001). Mechanisms of nutritional and hormonal regulation of lipogenesis. *EMBO Reports*, *2*(4), 282–286. https://doi.org/10.1093/embo-reports/kve071

Kim, J.-Y., van de Wall, E., Laplante, M., Azzara, A., Trujillo, M. E., Hofmann, S. M., Schraw, T., Durand, J. L., Li, H., Li, G., Jelicks, L. A., Mehler, M. F., Hui, D. Y., Deshaies, Y., Shulman, G. I., Schwartz, G. J., & Scherer, P. E. (2007). Obesity-associated improvements in metabolic profile through expansion of adipose tissue. *The Journal of Clinical Investigation*, *117*(9), 2621–2637. https://doi.org/10.1172/JCI31021

Klein, S. (2004). The case of visceral fat: Argument for the defense. *The Journal of Clinical Investigation*, *113*(11), 1530–1532. https://doi.org/10.1172/JCI22028

Lackey, D. E., Lynch, C. J., Olson, K. C., Mostaedi, R., Ali, M., Smith, W. H., Karpe, F., Humphreys, S., Bedinger, D. H., Dunn, T. N., Thomas, A. P., Oort, P. J.,

Kieffer, D. A., Amin, R., Bettaieb, A., Haj, F. G., Permana, P., Anthony, T. G., & Adams, S. H. (2013). Regulation of adipose branched-chain amino acid catabolism enzyme expression and cross-adipose amino acid flux in human obesity. *American Journal of Physiology. Endocrinology and Metabolism*, *304*(11), E1175-1187. https://doi.org/10.1152/ajpendo.00630.2012

Laeger, T., Reed, S. D., Henagan, T. M., Fernandez, D. H., Taghavi, M., Addington, A., Münzberg, H., Martin, R. J., Hutson, S. M., & Morrison, C. D. (2014). Leucine acts in the brain to suppress food intake but does not function as a physiological signal of low dietary protein. *American Journal of Physiology - Regulatory, Integrative and Comparative Physiology*, *307*(3), R310–R320. https://doi.org/10.1152/ajpregu.00116.2014

Lee, J. H., Park, A., Oh, K.-J., Lee, S. C., Kim, W. K., & Bae, K.-H. (2019). The Role of Adipose Tissue Mitochondria: Regulation of Mitochondrial Function for the Treatment of Metabolic Diseases. *International Journal of Molecular Sciences*, *20*(19). https://doi.org/10.3390/ijms20194924

Liu, Y., Dong, W., Shao, J., Wang, Y., Zhou, M., & Sun, H. (2017). Branched-Chain Amino Acid Negatively Regulates KLF15 Expression via PI3K-AKT Pathway. *Frontiers in Physiology*, *8*. https://doi.org/10.3389/fphys.2017.00853

Livak, K. J., & Schmittgen, T. G. (2001). Analysis of Relative Gene Expression Data Using RealTime Quantitative PCR and the 22DDCT Method. *Methods*, *25*, 402–408. https://doi.org/10.1006/meth.2001.1262

Luo, L., & Liu, M. (2016). Adipose tissue in control of metabolism. *Journal of Endocrinology*, *231*(3), R77–R99. https://doi.org/10.1530/JOE-16-0211

Mittal, B. (2019). Subcutaneous adipose tissue & visceral adipose tissue. *The Indian Journal of Medical Research*, *149*(5), 571–573. https://doi.org/10.4103/ijmr.IJMR_1910_18

Neinast, M., Murashige, D., & Arany, Z. (2019). Branched Chain Amino Acids. *Annual Review of Physiology*, *81*(1), 139–164. https://doi.org/10.1146/annurev-physiol-020518-114455

Nie, C., He, T., Zhang, W., Zhang, G., & Ma, X. (2018). Branched Chain Amino Acids: Beyond Nutrition Metabolism. *International Journal of Molecular Sciences*, *19*(4). https://doi.org/10.3390/ijms19040954

Ouchi, N., Parker, J. L., Lugus, J. J., & Walsh, K. (2011). Adipokines in inflammation and metabolic disease. *Nature Reviews Immunology*, *11*(2), 85–97. https://doi.org/10.1038/nri2921

Proteomics, C. (n.d.). *Branched Chain Amino Acids Analysis Service*. Creative Proteomics. Retrieved March 27, 2021, from https://www.creative-proteomics.com/services/branched-chain-amino-acids-analysis-service.htm

Ribeiro, R. V., Solon-Biet, S. M., Pulpitel, T., Senior, A. M., Cogger, V. C., Clark, X., O'Sullivan, J., Koay, Y. C., Hirani, V., Blyth, F. M., Seibel, M. J., Waite, L. M., Naganathan, V., Cumming, R. G., Handelsman, D. J., Simpson, S. J., & Couteur, D. G. L. (2019). Of Older Mice and Men: Branched-Chain Amino Acids and Body Composition. *Nutrients*, *11*(8). https://doi.org/10.3390/nu11081882

Saely, C. H., Geiger, K., & Drexel, H. (2012). Brown versus White Adipose Tissue: A Mini-Review. *Gerontology*, *58*(1), 15–23. https://doi.org/10.1159/000321319

Sanchez-Gurmaches, J., Hung, C.-M., & Guertin, D. A. (2016). Emerging Complexities in Adipocyte Origins and Identity. *Trends in Cell Biology*, *26*(5), 313–326. https://doi.org/10.1016/j.tcb.2016.01.004

Sethi, J. (2007). Thematic review series: Adipocyte Biology. Adipose tissue function and plasticity orchestrate nutritional adaptation. *Journal of Lipid Research*, *48*, 1253–1262. https://doi.org/10.1194/jlr.R700005-JLR200

Siddik, M. A. B., & Shin, A. C. (2019). Recent Progress on Branched-Chain Amino Acids in Obesity, Diabetes, and Beyond. *Endocrinology and Metabolism*, *34*(3), 234–246. https://doi.org/10.3803/EnM.2019.34.3.234

Siersbaek, R., Nielsen, R., & Mandrup, S. (2010). PPARgamma in adipocyte differentiation and metabolism—Novel insights from genome-wide studies. *FEBS Letters*, *584*(15), 3242–3249. https://doi.org/10.1016/j.febslet.2010.06.010

Sjögren, R. J. O., Rizo-Roca, D., Chibalin, A. V., Chorell, E., Furrer, R., Katayama, S., Harada, J., Karlsson, H. K. R., Handschin, C., Moritz, T., Krook, A., Näslund, E., & Zierath, J. R. (2020). Branched-Chain Amino Acid Metabolism is Regulated by ERRα and is Further Impaired by Glucose Loading in Type 2 Diabetes. *BioRxiv*, 2020.07.24.218099. https://doi.org/10.1101/2020.07.24.218099

Soliman, G. A. (2011). The integral role of mTOR in lipid metabolism. *Cell Cycle*, *10*(6), 861–862. https://doi.org/10.4161/cc.10.6.14930

Soliman, G. A., Acosta-Jaquez, H. A., & Fingar, D. C. (2010). MTORC1 inhibition via rapamycin promotes triacylglycerol lipolysis and release of free fatty acids in 3T3-L1 adipocytes. *Lipids*, *45*(12), 1089–1100. https://doi.org/10.1007/s11745-010-3488-y

Szymanski, M. W., & Singh, D. P. (2021). Isoproterenol. In *StatPearls*. StatPearls Publishing. http://www.ncbi.nlm.nih.gov/books/NBK526042/

Wang, J., Liu, Y., Lian, K., Shentu, X., Fang, J., Shao, J., Chen, M., Wang, Y., Zhou, M., & Sun, H. (2019). BCAA Catabolic Defect Alters Glucose Metabolism in Lean Mice. *Frontiers in Physiology*, *10*. https://doi.org/10.3389/fphys.2019.01140

Ye, Z., Wang, S., Zhang, C., & Zhao, Y. (2020). Coordinated Modulation of Energy Metabolism and Inflammation by Branched-Chain Amino Acids and Fatty Acids. *Frontiers in Endocrinology*, *11*, 617. https://doi.org/10.3389/fendo.2020.00617

Yoneshiro, T., Wang, Q., Tajima, K., Matsushita, M., Maki, H., Igarashi, K., Dai, Z., White, P. J., McGarrah, R. W., Ilkayeva, O. R., Deleye, Y., Oguri, Y., Kuroda, M., Ikeda, K., Li, H., Ueno, A., Ohishi, M., Ishikawa, T., Kim, K., … Kajimura, S. (2019). BCAA catabolism in brown fat controls energy homeostasis through SLC25A44. *Nature*, *572*(7771), 614–619. https://doi.org/10.1038/s41586-019-1503-x

Yoon, M.-S. (2016). The Emerging Role of Branched-Chain Amino Acids in Insulin Resistance and Metabolism. *Nutrients*, *8*(7). https://doi.org/10.3390/nu8070405

Zhang, F., Zhao, S., Yan, W., Xia, Y., Chen, X., Wang, W., Zhang, J., Gao, C., Peng, C., Yan, F., Zhao, H., Lian, K., Lee, Y., Zhang, L., Lau, W. B., Ma, X., & Tao, L. (2016). Branched Chain Amino Acids Cause Liver Injury in Obese/Diabetic Mice by Promoting Adipocyte Lipolysis and Inhibiting Hepatic Autophagy. *EBioMedicine*, *13*, 157–167. https://doi.org/10.1016/j.ebiom.2016.10.013

Zhao, X., Han, Q., Liu, Y., Sun, C., Gang, X., & Wang, G. (2016). The Relationship between Branched-Chain Amino Acid Related Metabolomic Signature and Insulin Resistance: A Systematic Review. *Journal of Diabetes Research*, *2016*, e2794591. https://doi.org/10.1155/2016/2794591